Brüel & Kjær

Technical Review

To Advance Techniques in Acoustical, Electrical, and Mechanical Measurement

Random load fatigue

No. 1 1968

PREVIOUSLY ISSUED NUMBERS OF BRÜEL & KJÆR TECHNICAL REVIEW

TECHNICAL REVIEW

No. 1 — 1968

Peak Distribution Effects in Random Load Fatigue

By *Jens Trampe Broch,* Dipl. ing. E.T.H.

ABSTRACT

In describing random processes one normally starts by stating the first order probability density function. To further specify the process use is sometimes made of higher order probability distributions. One such "higher order" distribution function is the probability function for the number of maxima (or minima) per unit time i.e. the distribution function for the process reversals. This distribution function is commonly termed the process *peak distribution.*

The aim of the studies reported in this paper has been to investigate the effects of the stress peak distribution upon the fatigue life of a certain type of test specimen excited to bending by Gaussian random vibrations. Approximately 200 specimens were tested using two different peak distribution functions. The peak distribution functions were produced by means of a one and two degrees of freedom system, respectively, excited by bands of random noise.

The RMS-level of the strain as well as the average number of zero crossings were kept constant and equal in both tests. Statistical and physical interpretations of the test results are presented and discussed.

SOMMAIRE

Pour décrire des phénomènes aléatoires, on commence normalement par en donner la fonction de densité de probalité du premier ordre. En vue d'apporter plus de précision sur le phénomène, il est parfois fait usage de distributions de probabilité d'ordre supérieur. Une de ces fonctions de distribution d'ordre «supérieur» est la fonction de probabilité relative au nombre de maxima (ou minima) par unité de temps, c'est-à-dire la fonction de distribution qui concerne les changements de sens dans le déroulement du processus. On l'appelle habituellement la fonction de *distribution des crêtes* du processus.

Le but des études dont il est question dans ce papier était d'explorer les effets de la distribution des crêtes de la sollicitation sur la longévité d'un certain type d'éprouvettes excité en flexion par des vibrations aléatoires gaussiennes. Deux cents spécimens environ ont été essayés en utilisant deux fonctions différentes de distribution de crête. Les fonctions de distribution de crête ont été produites au moyen d'un système à un ou deux degrés de liberté, l'un et l'autre excités par des bandes de bruit aléatoire.

Le niveau en valeur efficace de la contrainte, tout comme le nombre moyen de passages par zéro, ont été tenus constants et égaux dans les deux essais. Des interprétations statistiques et physiques des résultats des essais sont présentées et discutées.

ZUSAMMENFASSUNG

Die Beschreibung eines stochastischen Vorgangs beginnt normalerweise mit einer Aussage über die statistische Verteilung der Momentanwerte (Wahrscheinlichkeitsdichte des Momentanwerts). Um den Vorgang näher zu kennzeichnen, gibt man manchmal auch die Verteilung für weitere Kennwerte der Zeitfunktion an. Eine solcher Angaben betrifft die Wahrscheinlichkeitsdichte, mit der die Maxima (oder Minima) über den Amplitudenbereich verteilt sind, d. h. die statistische Verteilung der Richtungsumkehrungen. Diese Verteilung wird gemeinhin als *Spitzenverteilung* des Vorgangs bezeichnet.

Die Untersuchungen, von denen in diesem Aufsatz berichtet wird, hatten das Ziel, die Wirkung der Spitzenverteilung der mechanischen Spannung auf die Lebensdauer eines bestimmten Typs von Prüfobjekten zu erforschen, die durch stochastische Schwingungen mit Gauß'scher Momentanwertverteilung zu Biegeschwingungen angeregt wurden. Etwa 200 Objekte wurden mit zwei verschiedenen Spitzenverteilungen geprüft. Die Spitzenverteilungen wurden erzeugt, indem Schwingsysteme mit 1 bzw. 2 Freiheitsgraden durch Rauschbänder angeregt wurden.

Der Effektivwert der Dehnung wie auch die mittlere Frequenz der Nulldurchgänge wurden konstant und für beide Spitzenverteilungen gleich groß gehalten.

Statistische und physikalische Deutungen der Prüfergebnisse werden vorgestellt und erörtert.

Introduction

Structural vibrations encountered in practice are normally a combination of several mechanical oscillations acting together and giving a more or less complicated displacement versus time trace. If, for instance, the displacement of a particular point of a particular structural member of an aircraft in flight is plotted as a function of time the result may well be a curve of the type shown in Fig. 1. The actual vibration at the point of observation is here caused not only by the complex forces loading the airframe but also by resonance effects in structural members transferring these forces to the observation point. Similar vibration traces may be found from measurements on cars moving along rough roads, ships moving in rough waters, complex building structures responding to unsteady winds, etc.

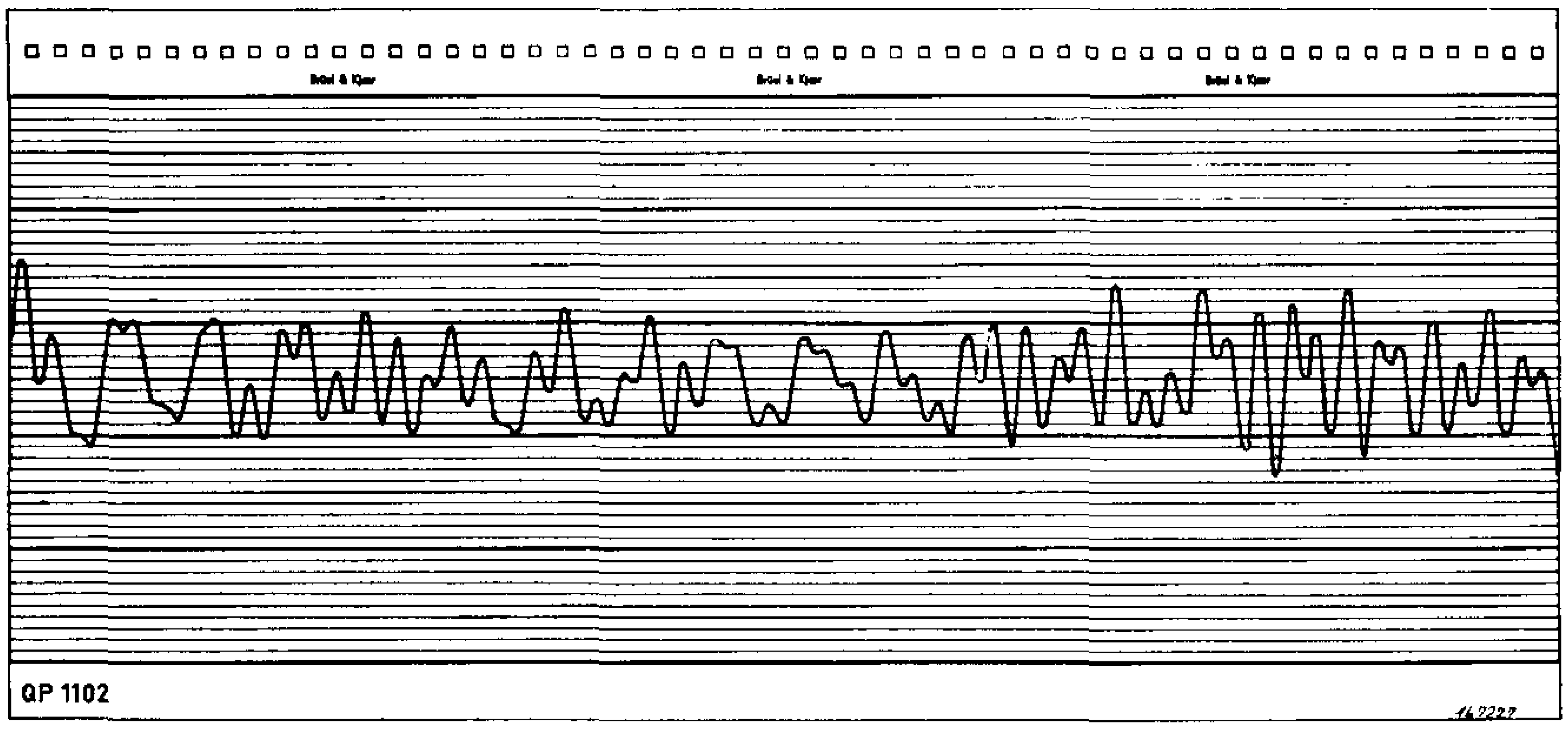

Fig. 1. Typical displacement versus time trace for a particular point on a randomly excited complex structure.

Vibrations of the kind shown in Fig. 1 cannot be conveniently described in deterministic terms but must be treated on a statistical or probabilistic basis. While the characteristics of simple periodic motion are known when one period of motion is known the exact future amplitude of the vibration signal, Fig. 1, cannot be predicted even if its complete history is known. It is, however, possible to determine the probability of finding instantaneous amplitude values within a narrow amplitude window, Δx, see Fig. 2. As the probability of finding amplitude values within Δx will depend upon the width of the window it has been found more convenient for a description to use the concept of *probability density* instead of probability. The probability density is found by dividing the probability of finding amplitude values within Δx by Δx:

$$p(x) = \lim_{\Delta x \to 0} \frac{P(x, x + \Delta x)}{\Delta x}$$

where

$$P(x, x + \Delta x) = \frac{\Sigma \Delta t_n}{T}$$

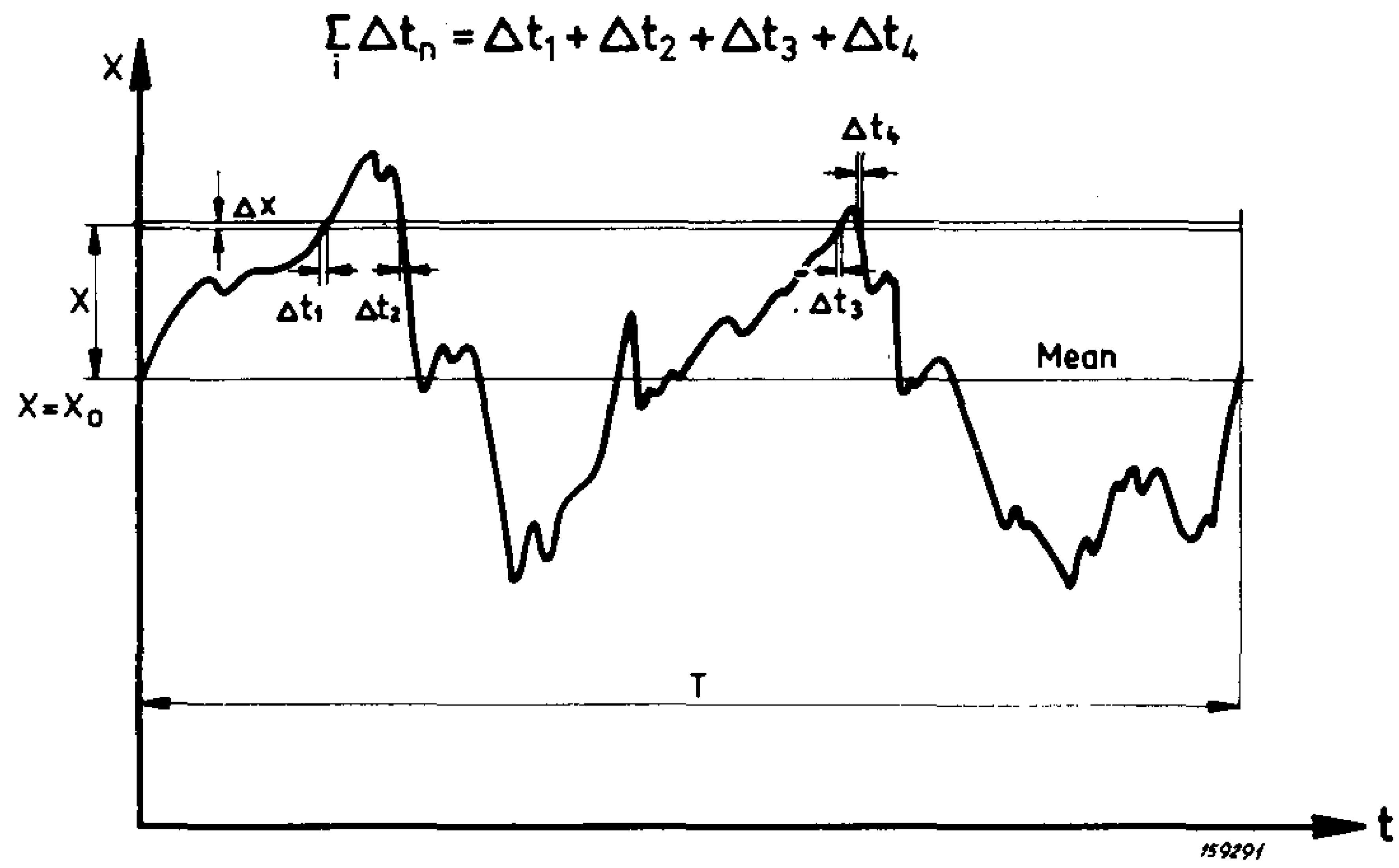

Fig. 2. Sketch illustrating the concepts of probability and probability density on the basis of a moveable amplitude "window", Δx, situated at the level x.

By varying the value of x from $-\infty$ to $+\infty$ and plotting $p(x)$ as a function of x the probability density curve for instantaneous amplitude values of the vibrations is found.

The shape of this curve may vary considerably depending upon the nature of the applied forces as well as upon possible amplitude nonlinearities in the structural responses. However, the most well known probability density curve is that obtained from a normal (Gaussian) random process, see Fig. 3.

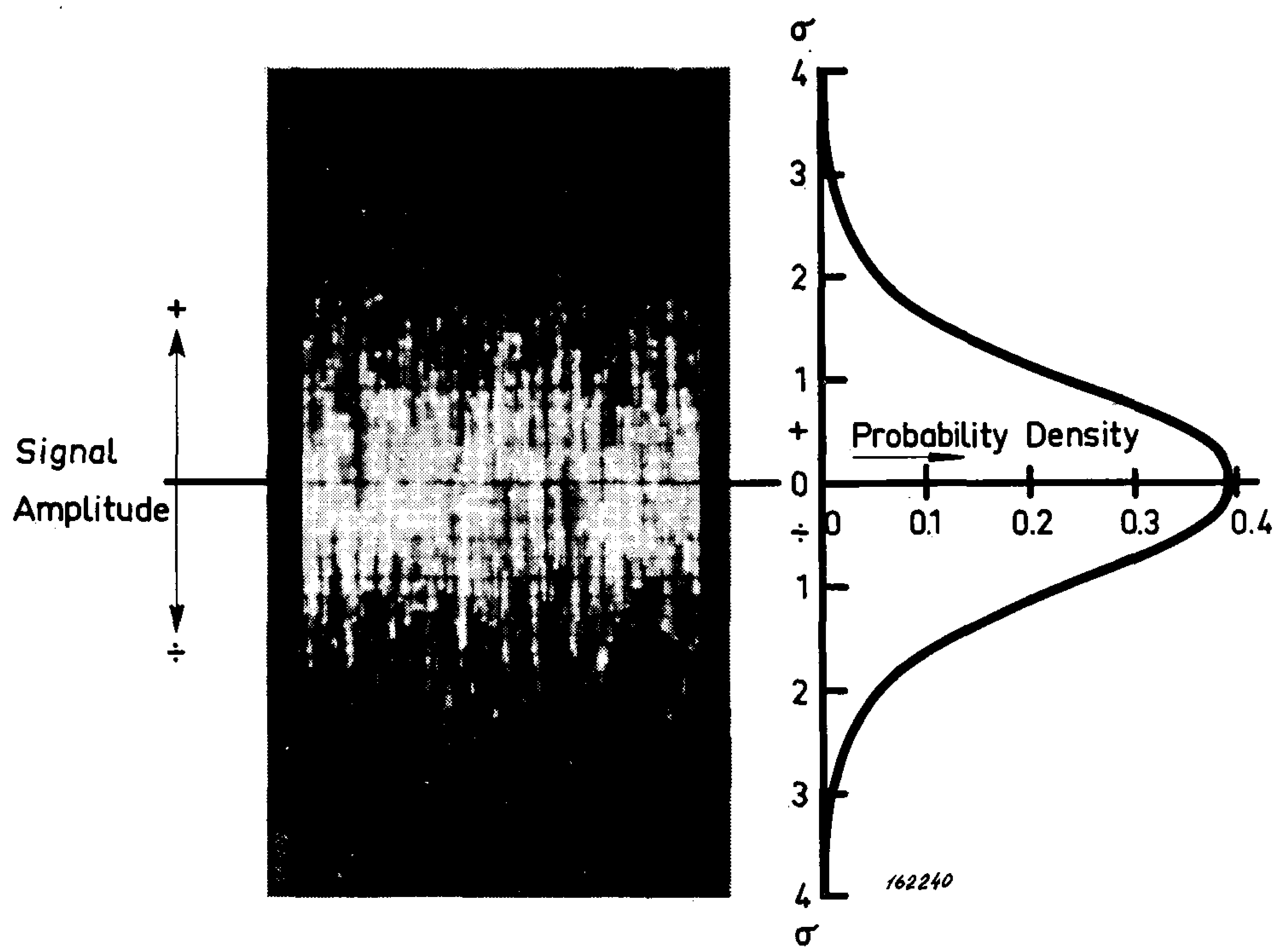

Fig. 3. Illustration of the relationship between the instantaneous amplitude values in a Gaussian random vibration signal and the Gaussian probability density curve.

Probability density curves obtained in the manner described above are often termed *first order probability density curves* because they do not depend upon the actual behaviour of the vibration signal before (or after) it passes through the narrow amplitude window, Δx, in Fig. 2. If, on the other hand, certain restrictions are formulated as to the behaviour of the signal also when it is outside Δx the curves obtained are commonly designated as higher order probability density functions.

One such "higher order"*) probability density function is the probability

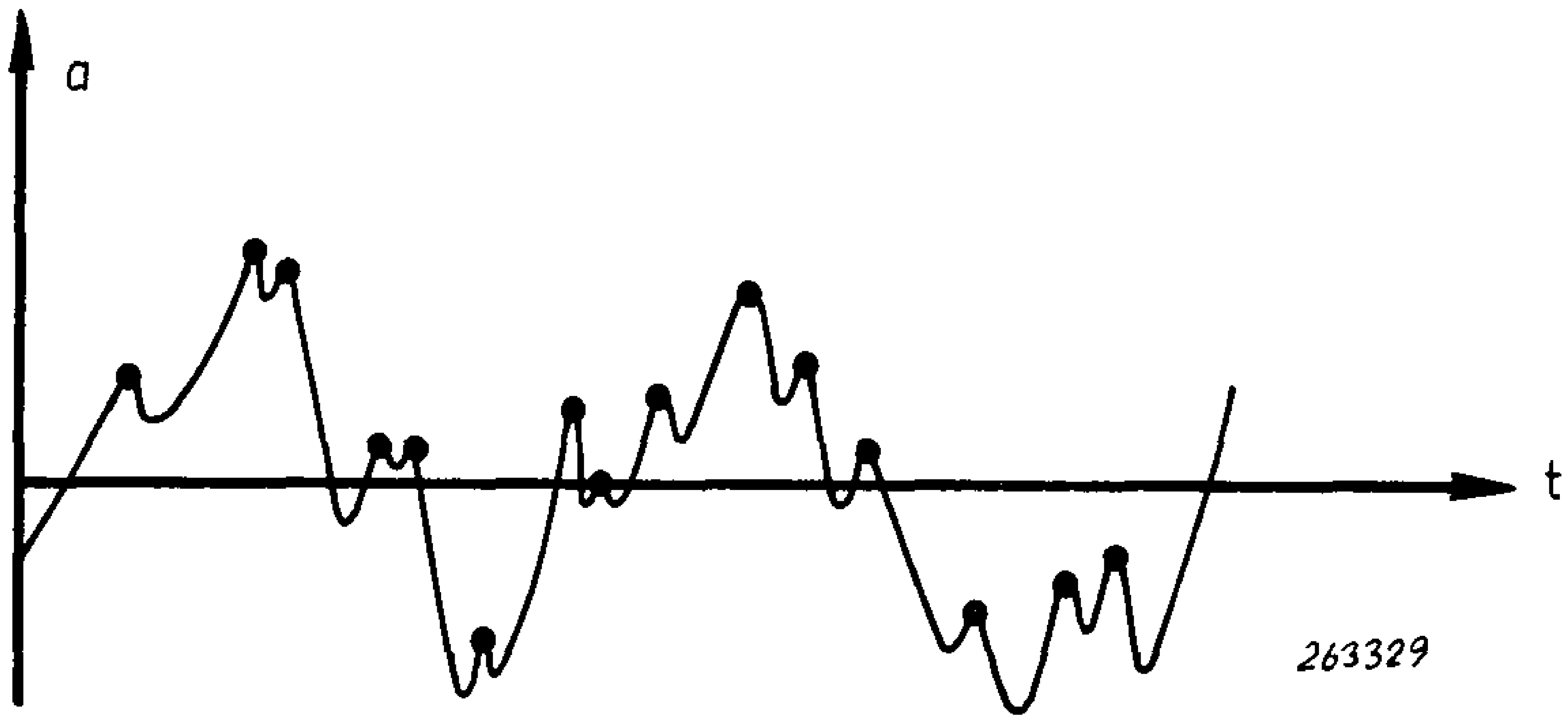

Fig. 4. Sketch illustrating the distribution of maxima in a random vibration signal.

density function for the vibration maxima, Fig. 4, because it restricts the observations on the signal inside Δx to cases where the magnitude of the signal is smaller than x both immediately before the signal enters the window and immediately after it leaves it again. By plotting the number of maxima inside Δx per unit time as a function of signal level, x, a curve proportional to the probability density curve for the vibration maxima is obtained. When this curve is normalized to unit area it is commonly termed the *peak probability density curve.*

Other higher order probability functions describing randomly varying vibration signals can be derived. In general, however, the use of these higher order probability functions is rather complicated and they describe the signal in the form of probability density surfaces rather than curves. The two probability density functions discussed above, i.e. *the first order probability density curve* and *the peak probability density curve,* are relatively easy to measure and are therefore especially attractive to use in the description of random processes.

Random Load Fatigue

The fatiguing of engineering materials when these are subjected to alternating stresses has been studied for more than 100 years. However, because so

---

*) The inverted commas on the term "higher order" are used here because in most textbooks on probability theory a somewhat different definition is given to higher order probability density functions. The meaning of the term, however, as explained in the text, remains the same.

many different factors may influence the fatigue life of a particular structural element, and because it is realized that the fatigue process in itself is of a statistical nature, no unique method for the prediction of mechanical fatigue has as yet been developed. A number of so-called "cumulative damage rules" have been suggested in the past, the most well known of these being the Palmgren-Miner hypotheses, but none of these rules seem to be generally applicable to common service loads. Without going into details it seems reasonable here, however, to summarize briefly some recent findings on the physical nature of the fatigue of metals. The findings cited have developed mainly from the field of aircraft material research where fatigue problems are a major concern.

Even though it is believed that the production of microscopic slip bands in the initial portion of the fatigue process is caused by an interaction between spatial stress concentrations and submicroscopic crystal dislocations in the material no concise proof for this theory seems to exist today. On the other hand, when the slip bands have formed they are observed to progress and form minute cracks which eventually join together and produce major cracks. These cracks then propagate in the material until a final stage of crack instability and catastrophic failure is reached.

While the crack initiation process as well as the final crack instability and failure stages are highly statistical in nature the crack propagation process seems to follow laws of a more deterministic character. Taken as a whole, however, fatigue failure must be regarded as a statistical phenomenon as suggested by Weibull in the nineteen forties.

In addition to fatigue crack initiation and propagation studies a number of investigators have also studied the statistical distribution of fatigue endurances at various stress levels. Out of these studies an hypothesis has been formed that two different fatigue "mechanisms" govern the fatigue life of a particular material, one "mechanism" acting at low stress levels and another "mechanism" acting at high stress levels. Furthermore, the transition from one "mechanism" to the other is supposed to take place gradually with stress level. A fact which seems to support this theory is that some materials show a more or less distinct "bend" in the fatigue life curve (S–N-curve) at a certain stress level.

The S–N-curve referred to above is a curve indicating the peak amplitude of a sinusoidal stress function versus the number of cycles to failure, see Fig. 5. Such curves are often published by material manufacturers together with other relevant material data. The conditions under which the curves were obtained are (unfortunately) not always stated by the supplier. One condition is, however, in general fulfilled: the curves have been obtained from tests with zero mean stress, i.e. they refer to purely sinusoidal loading of the material. As soon as nonzero, or varying, mean stresses are superimposed upon the pure sinusoidal loading other types of curves may eventually develop. The curve shown in Fig. 5 has been reproduced from a materials handbook and the "bend" in the curve mentioned above is clearly noticed.*) If the test specimen is loaded by a forcing function which is *not* purely sinusoidal, for instance a forcing function of the type shown in Fig. 1, material data in the form of conventional S–N-curves are not immediately applicable. First of all the peak amplitude of the curve Fig. 1, varies irregularly with time, and secondly the concept of "cycle" may be difficult to define.

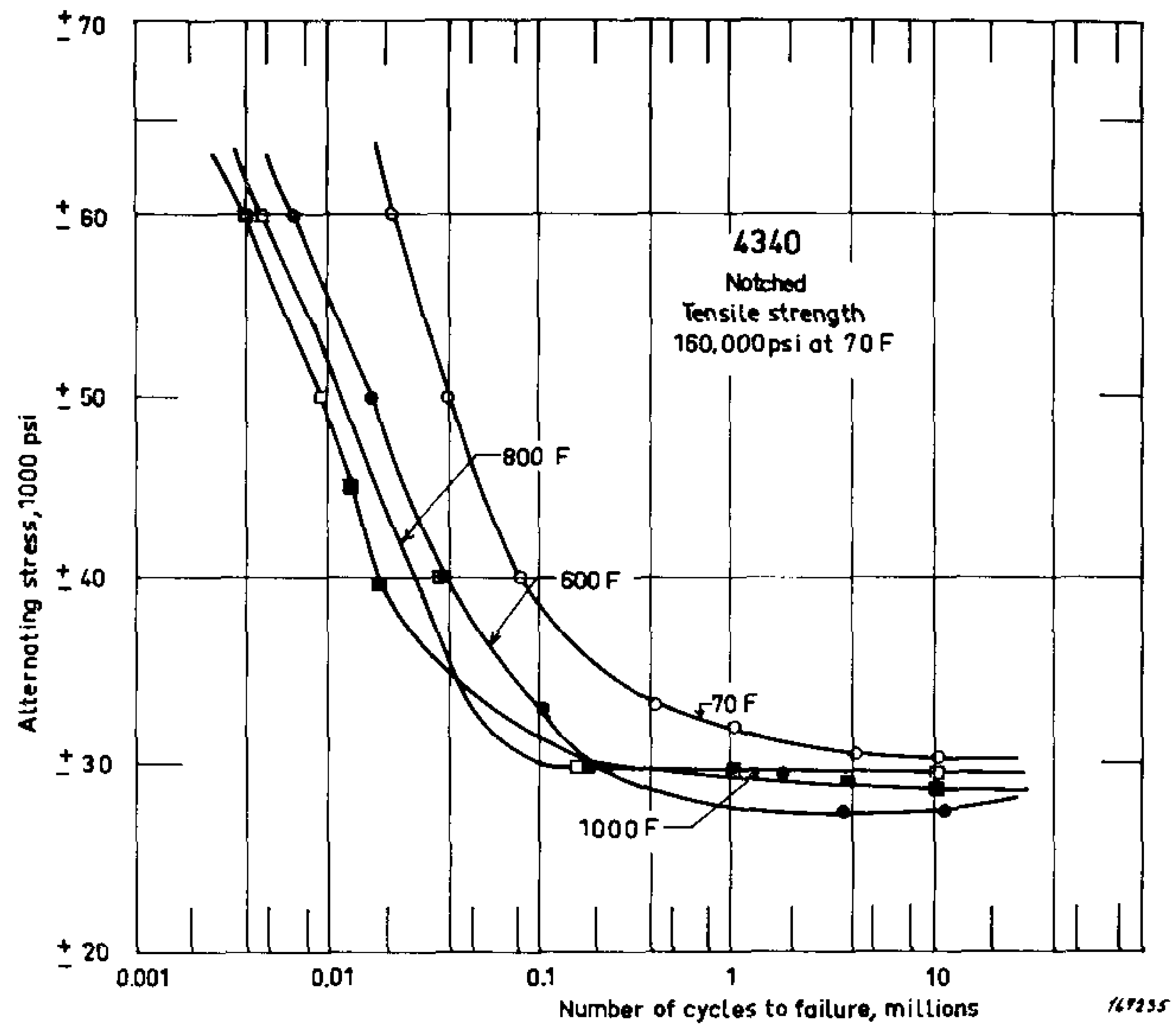

Fig. 5. Fatigue strength curves for notched 4340 steel. (From "Metals Handbook").

Even though some sort of "cycle", or frequency, may be defined in a statistical sense (this is further discussed later in the paper) the correlation from "cycle" to "cycle" is widely different from that of a pure sinusoid. Also, as the stress reversals (peaks) occur at a variety of stress levels this would cause complicated interactions between the two fatigue "mechanisms" (assuming that the "two fatigue mechanism hypothesis" is valid!).

Altogether, the problem of random load fatigue is a very complicated one and a considerable amount of research remains to be done before definite knowledge in this area is obtained, which can ultimately be developed into better fatigue life predictions and design rules. An attempt to approach some of the problems in a phenomenological way is described in this paper and it is hoped that this in conjunction with some earlier work of the author, may contribute to further such a development.

Load Spectra and Peak Distributions

If an amplitude versus time signal of the type shown in Fig. 1 is FOURIER analyzed (i.e. converted from a description in the time domain to a description in the frequency domain) it will, in general, show a continuous frequency spectrum. Examples of such spectra are shown in Fig. 6.

*) Not all engineering materials show this distinct "bend". In some cases the "bend" consists of a very gradual decrease in slope of the curve with decreasing peak stresses.

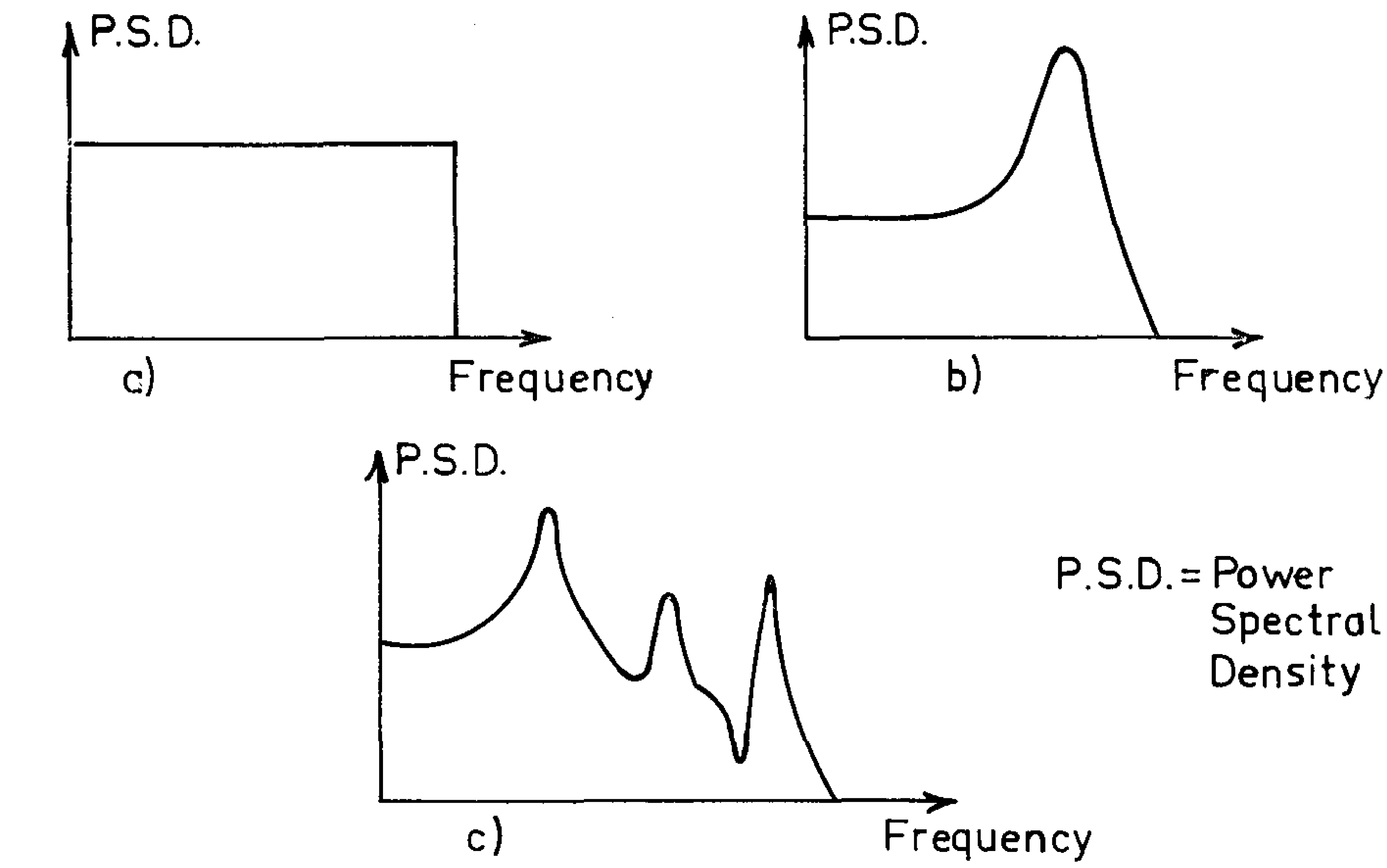

Fig. 6. Examples of continuous frequency spectra:
a) Spectrum with constant power spectral density.
b) Spectrum indicating the existance of a single resonance.
c) Spectrum indicating that more than one resonance effect is present.

It should be noted at this stage that in the introduction to this paper the signal, Fig. 1, was described in terms of probability density functions while at this point another method of description, the frequency spectrum method, has been introduced. This might, at first glance, seem a little confusing. However, both methods of description are in this case based on statistical characteristics of the signal and supplement each other in an excellent way.

As S. O. Rice and others have shown signals which exhibit Gaussian (normal) first order probability density characteristics can be represented by an infinite number of sine waves combined in random phase, i.e. by continuous frequency spectra. He has also shown that when the signal exhibits a Gaussian first order probability density characteristic the frequency spectrum *defines* the signal in a statistical sense so that higher order probability density functions are, in principle, derivable from the signal frequency spectrum. This means that in the case of Gaussian random vibrations the peak probability density curve depends directly upon the signal frequency spectrum.

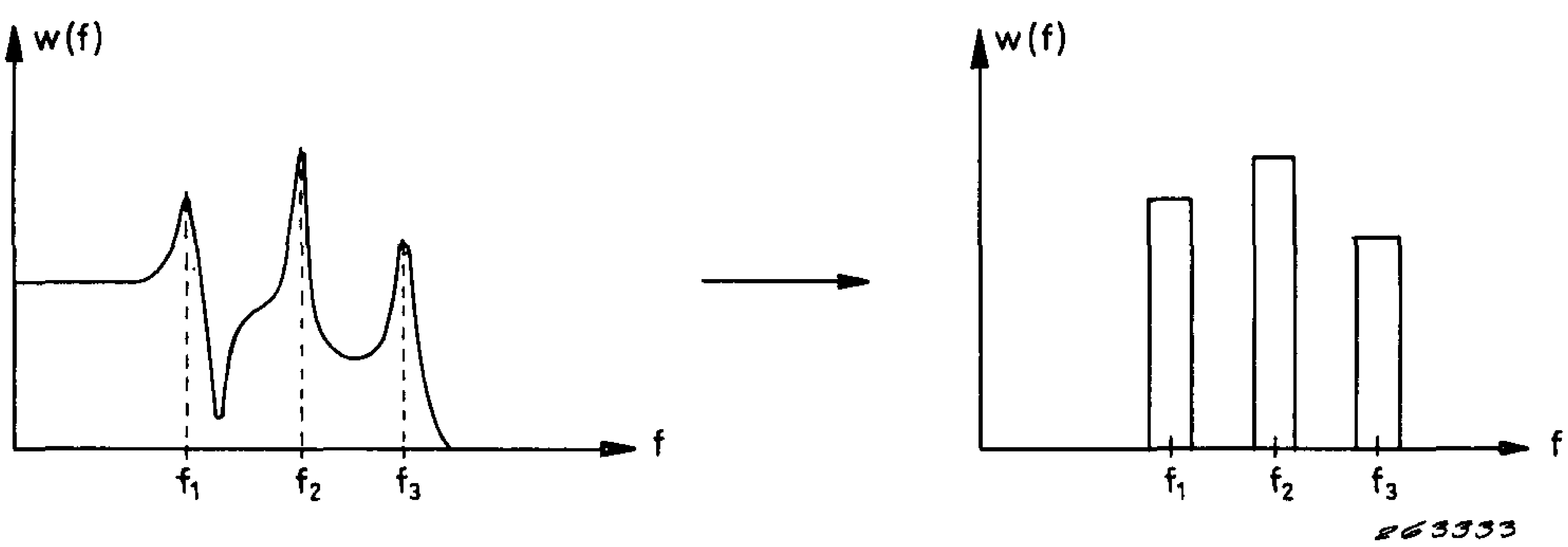

Fig. 7. Illustration of the "box"-theory.

Based upon the work of Rice the author, in some earlier work, investigated this relationship and developed an approximate theory which allowed for an easy estimation of the peak probability density curve when the signal frequency spectrum was known. This theory was termed the "box"-theory*)

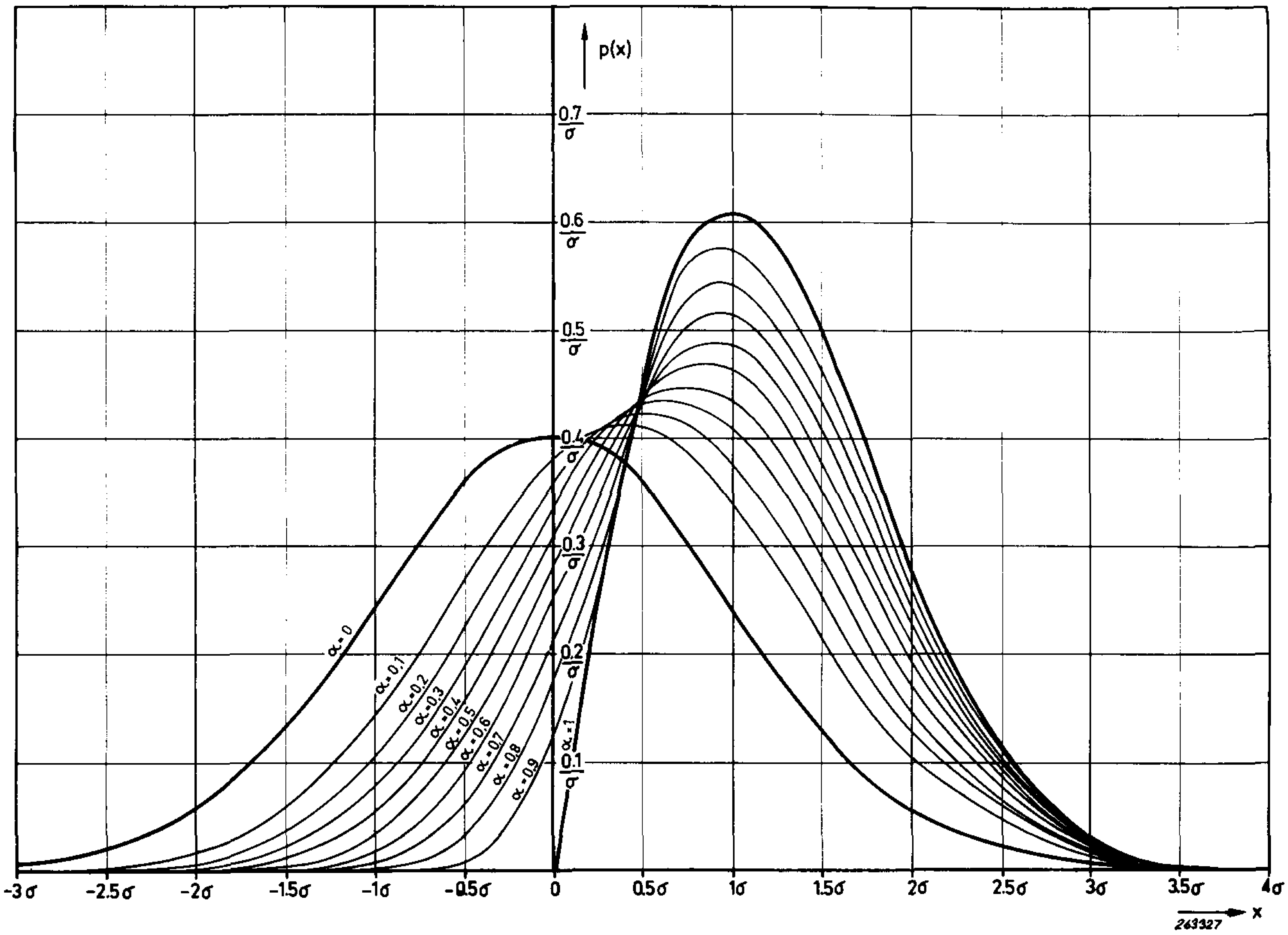

Fig. 8. Set of normalized peak probability density curves plotted with α as parameter.

because resonance peaks in the vibration frequency spectrum were approximated in the form of "boxes", see Fig. 7. From these "boxes" it is an easy matter to calculate a factor, α, which determines the shape of the peak probability density curve, Fig. 8.

The formula obtained for α in the case of a multi degree-of-freedom system is:

$$\alpha = \frac{\left[1 + \sum_n \left(\frac{f_n}{f_1}\right)^2 \times \beta_n\right]^2}{\left[1 + \sum_n \beta_n\right]\left[1 + \sum_n \left(\frac{f_n}{f_1}\right)^4 \times \beta_n\right]}$$

where: f_1 = center frequency of first resonance

f_n = center frequency of the n'th resonance ($n > 1$)

$$\beta_n = \frac{c_n}{c_1} \times \frac{\Delta f_n}{\Delta f_1}$$

*) "Effects of Spectrum Non-linearities upon the Peak Distribution of Random Signals". Brüel & Kjær Techn. Rev. No. 3 - 1963.

$\frac{c_n}{c_1}$ = energy-ratio between the maximum responses of the two resonances (energy-ratio of the corresponding spectrum peaks)

Δf_1 = −3 dB bandwidth of the first resonance peak

Δf_n = −3 dB bandwidth of the n'th resonance peak

As can be seen from the formula the spectrum defines the peak probability density curve, while the converse is not true, i.e. the peak probability density curve does *not* define the spectrum. Said in other words: different frequency spectra may produce the same peak probability density curve. The two functions discussed in the introduction, the first order probability density function and the peak probability density function, may therefore not be sufficient to describe a signal of the type shown in Fig. 1 with regard to its mechanical damage producing potential. However, when they are considered in conjunction with the vibration frequency spectrum certain trends may be found which might produce fruitful results. One could, of course, argue that a determination of the peak probability density curves is not necessary because the information is already contained in the signal frequency spectrum. There are, on the other hand, several reasons why it is desirable to also determine this curve. Firstly it gives certain information as to *how,* on the average, the vibration peaks are distributed over the signal amplitude values. Secondly it might, from fatigue experiments of the kind discussed later in the text, turn out that only certain α-values need to be regarded in fatigue life estimates. Finally, when amplitude non-linearities exist in the vibrating system, so that the first order probability density function is no longer Gaussian, the peak probability density curve cannot be calculated directly from the vibration frequency spectrum and a determination of this curve will consequently furnish additional *new* information about the signal.

Some Experimental Test Considerations

The experiments described in the following have been designed to investigate the effect of a complex, random stress history upon the fatigue life of a certain type of test specimen excited to bending. Two types of stress versus time functions were used for the purpose and samples of these functions are shown in Fig. 9. (Actually the signals shown in Fig. 9 were obtained from strain measurements using resistive wire strain gages. Assuming that a linear stress-strain relationship exists in this case, however, the signals will also represent the stress versus time functions.) The function plotted in Fig. 9a) was obtained by arranging the test specimen so that it acted as a single degree-of-freedom resonant system and exciting it mechanically by means of an electro-dynamic vibrator, Fig. 10. The vibrator was fed with a narrow band of Gaussian random noise centered at the system resonance frequency.

In the case of the signal Fig. 9b) the test specimen was arranged to form a two degree-of-freedom system, Fig. 11, and two bands of random noise were used to feed the vibrator.

The bandwidths of the exciting noise signals were chosen to be wide enough

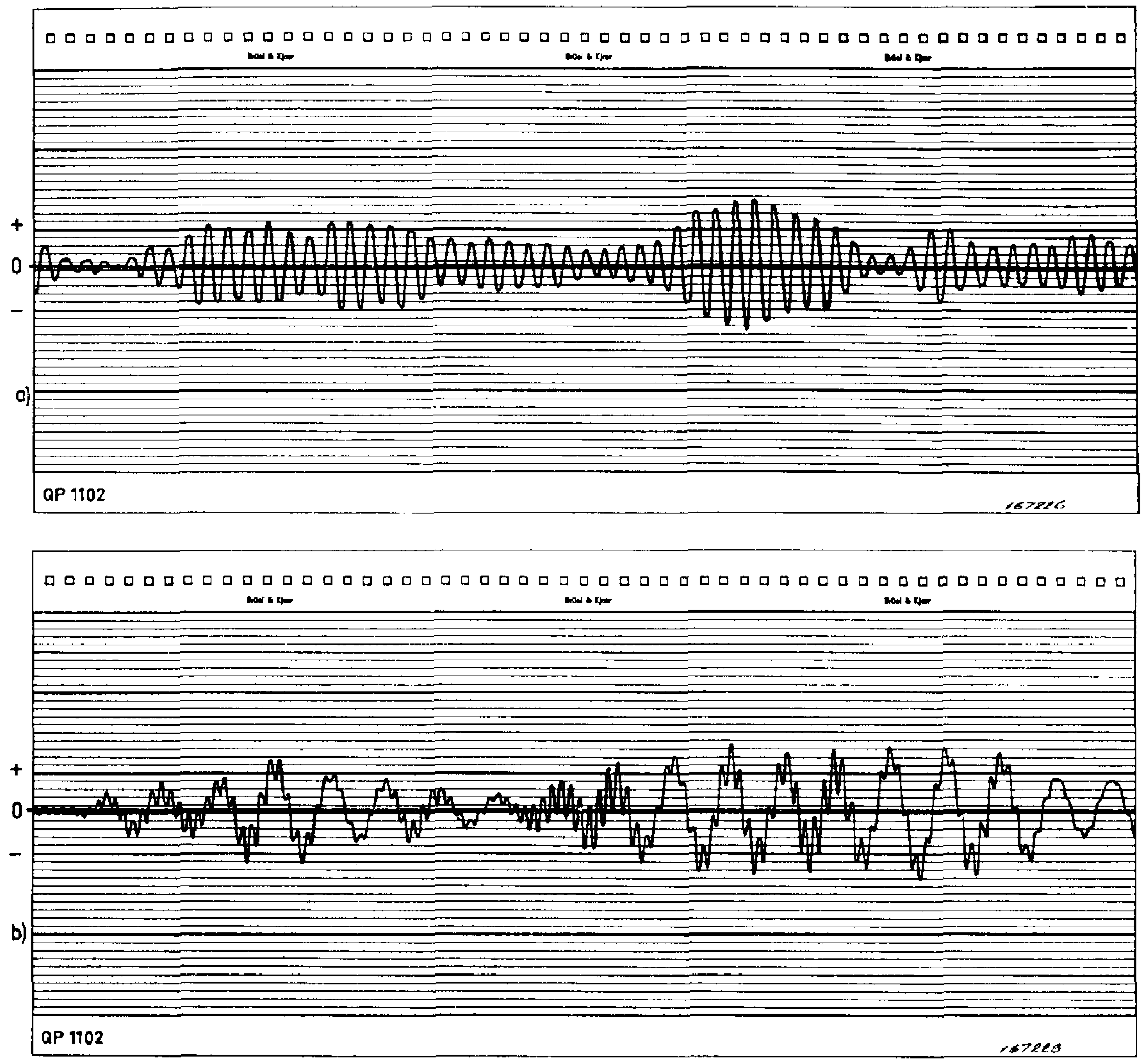

Fig. 9. Amplitude versus time functions for the stresses in the specimens.
a) Sample obtained from measurements on the single degree-of-freedom test system.
b) Sample obtained from measurements on the two degrees-of-freedom system.

to allow for slight changes in resonance frequency of the test system during testing. Two very important considerations had to be taken into account in designing the experiments:

1. The RMS strain (or stress) level should be the same in both cases (Fig. 9a and Fig. 9b).
2. The average number of zero crossings ("average" frequency) was to be kept the same in both tests.

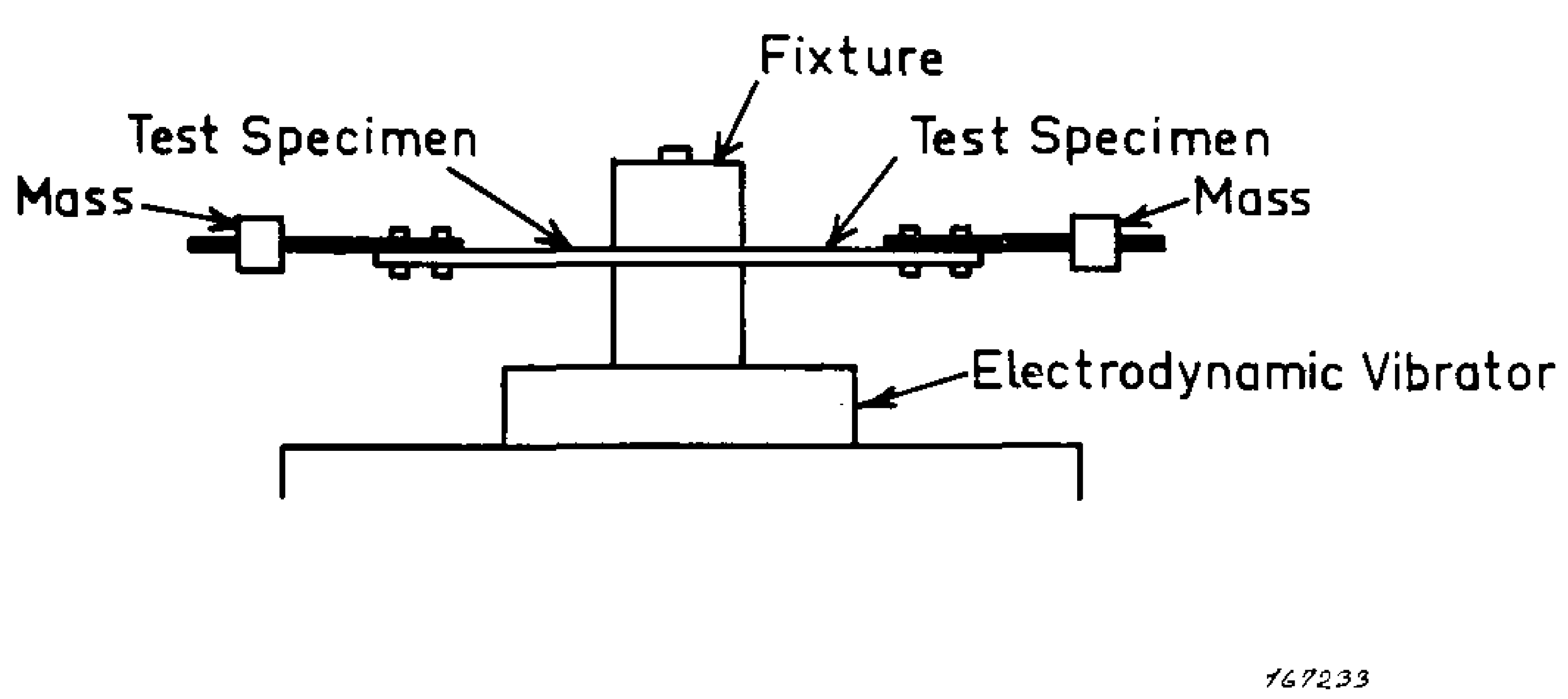

Fig. 10. Sketch of the specimen arrangement used in the single degree-of-freedom test. (Actually two symmetrically mounted single degree-of-freedom systems are shown).

The reason for these requirements is that the actual number of high stress peaks (above say 2 σ, where σ = RMS-value) will then be the same in the two cases,*) and the only difference between the two stress signals will be the *distribution* of the stress reversals, i.e. their α-value.
For the single degree-of-freedom system the average number of zero crossings is simply equal to the resonance frequency and the only "adjustment" necessary is to set the desired RMS strain level.
In the case of the two degree-of-freedom system the average number of zero-crossings depends upon the actual resonance frequencies as well as upon the ratio between the two resonant responses. Also in this case the previously mentioned "box"-theory allows a simple estimate of the relationship, see Appendix A.
When the two resonance frequencies have been adjusted (mechanically) to their desired values the system is excited to a low vibration level, first by one band of noise only and then by the second band of noise only. The strain responses in the two cases are noted and the excitation adjusted until the desired response ratio is reached. Then both bands of noise are applied simultaneously and the total excitation level increased to the correct test level (RMS-strain response level). The average number of zero-crossings can be

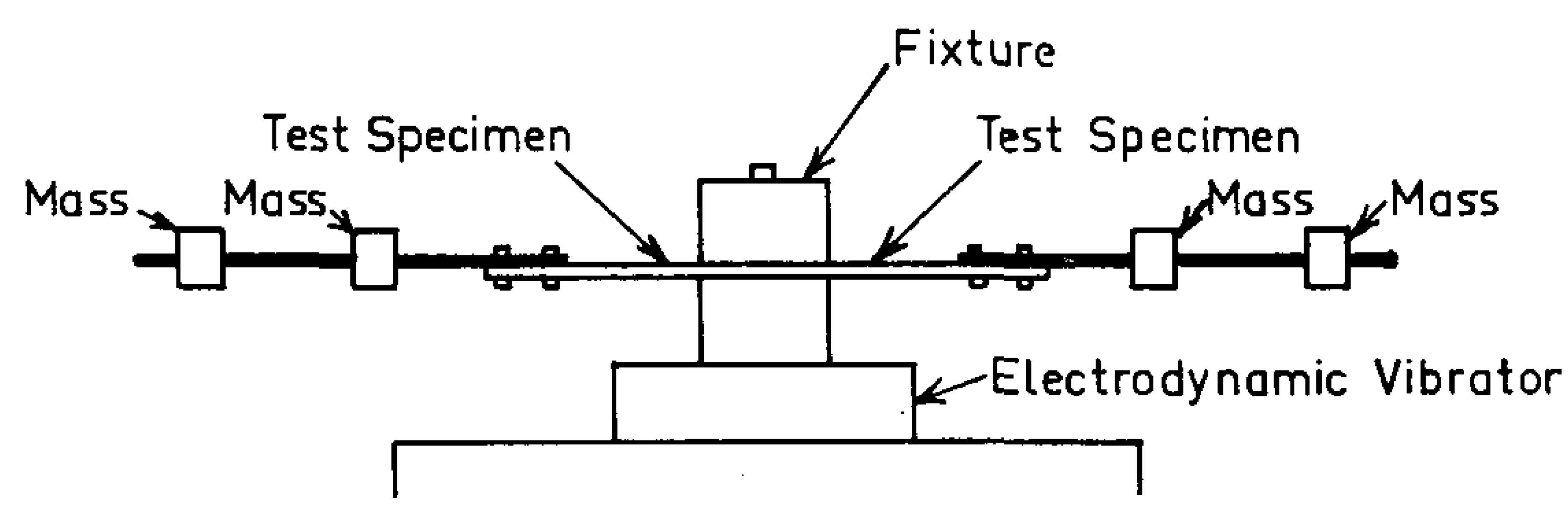

Fig. 11. Sketch of the specimen arrangement used in the two degrees-of-freedom test. (Two symmetrically mounted specimens are shown).

checked by means of an electronic counter and the "high" frequency excitation slightly "corrected" until the appropriate value is obtained.
Typical frequency spectrum recordings of the strain are shown in Fig. 12. The RMS test level was, on the basis of some pilot experiments chosen in such a manner that the initial setting-up and "correction" period should be small compared with the average time to failure. On the other hand, each test run should preferably be finished within a normal, or a not too extended, working day. Also, the dynamic load should be of such a magnitude that the difference in static loading between the two cases investigated due to differences in mass loads was as small as possible. A check on these loads showed that the difference in static loading was of the order of 10 % of the RMS-value of the dynamic load. The possible consequence of this difference is discussed in the section "Evaluation of the Test Results".

*) See Appendix B.

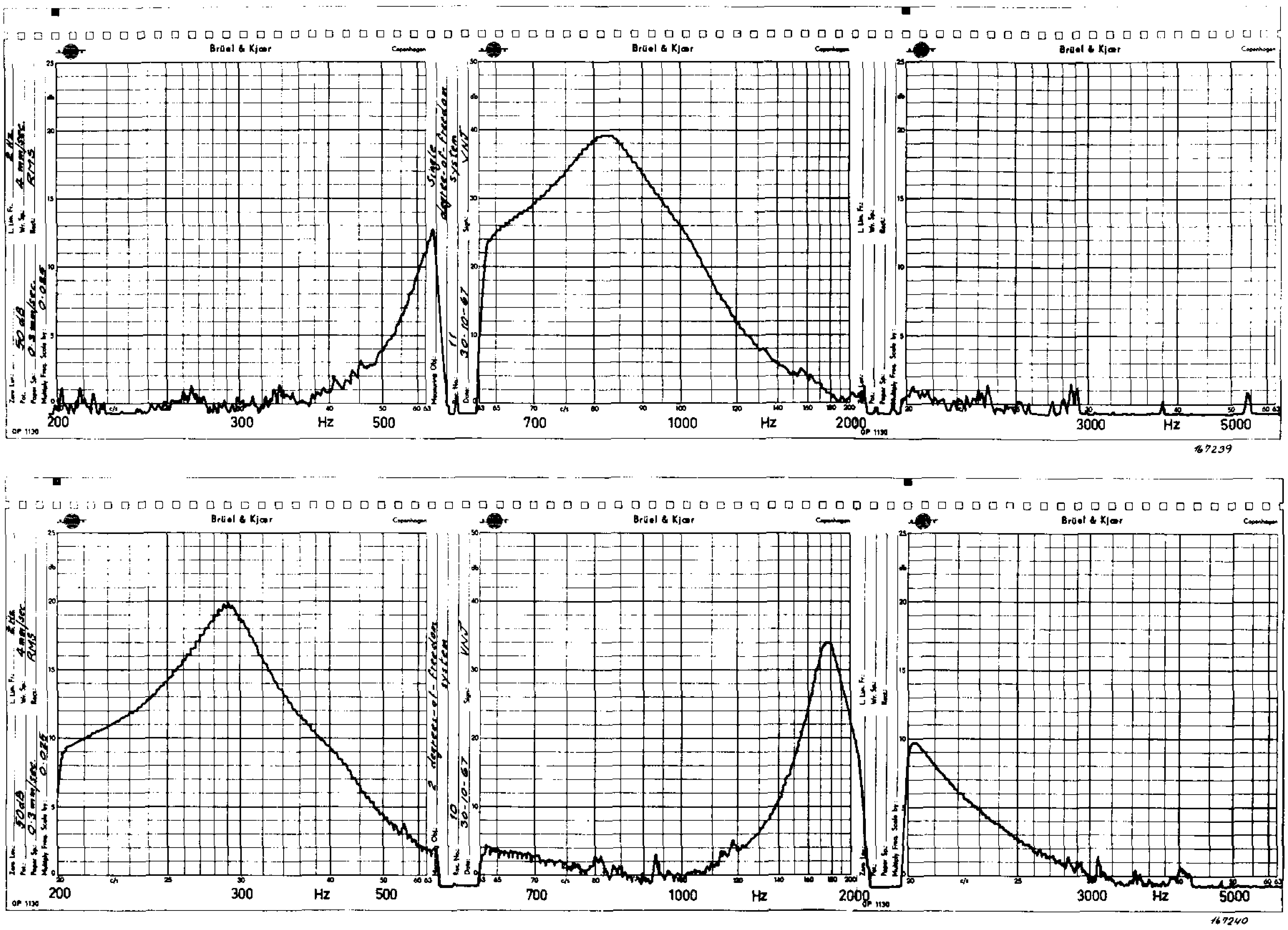

Fig. 12. Typical frequency spectra of the strain in the test specimens during testing.

a) Spectrum obtained from measurements on the single degree-of-freedom test system.

b) Spectrum obtained from measurements on the two degrees-of-freedom test system.

The spectra were obtained from magnetic tape recordings of the strain and frequency analyzed after a forty to one tape speed transformation. The actual resonance frequencies were 20.5 Hz in case a) and 7.3 Hz and 44 Hz in case b). Analysis bandwidth: 6 % (B & K Type 2107).

Due to the statistical nature of fatigue it was clear that a large number of specimens had to be tested to obtain statistically significant trends in the results. Furthermore, some sort of automatic detection of failure was necessary to avoid continuous supervision, and the specimen shape should be such that failure occurred at a well defined spatial point. As the tests were designed to be comparative rather than absolute the actual material used to produce the specimen from was, in the first instance, of little consequence. These considerations led to the use of epoxy paper printed circuit boards, notched to produce stress concentrations, Fig. 13. The notch was produced by drilling and rolling to "pre-damage" the specimen as little as possible.

From measurements of the dynamic modulus of elasticity and the mechanical loss factor of a large number of boards by means of a Complex Modulus Apparatus Type 3930 it was concluded that their responses to vibration were

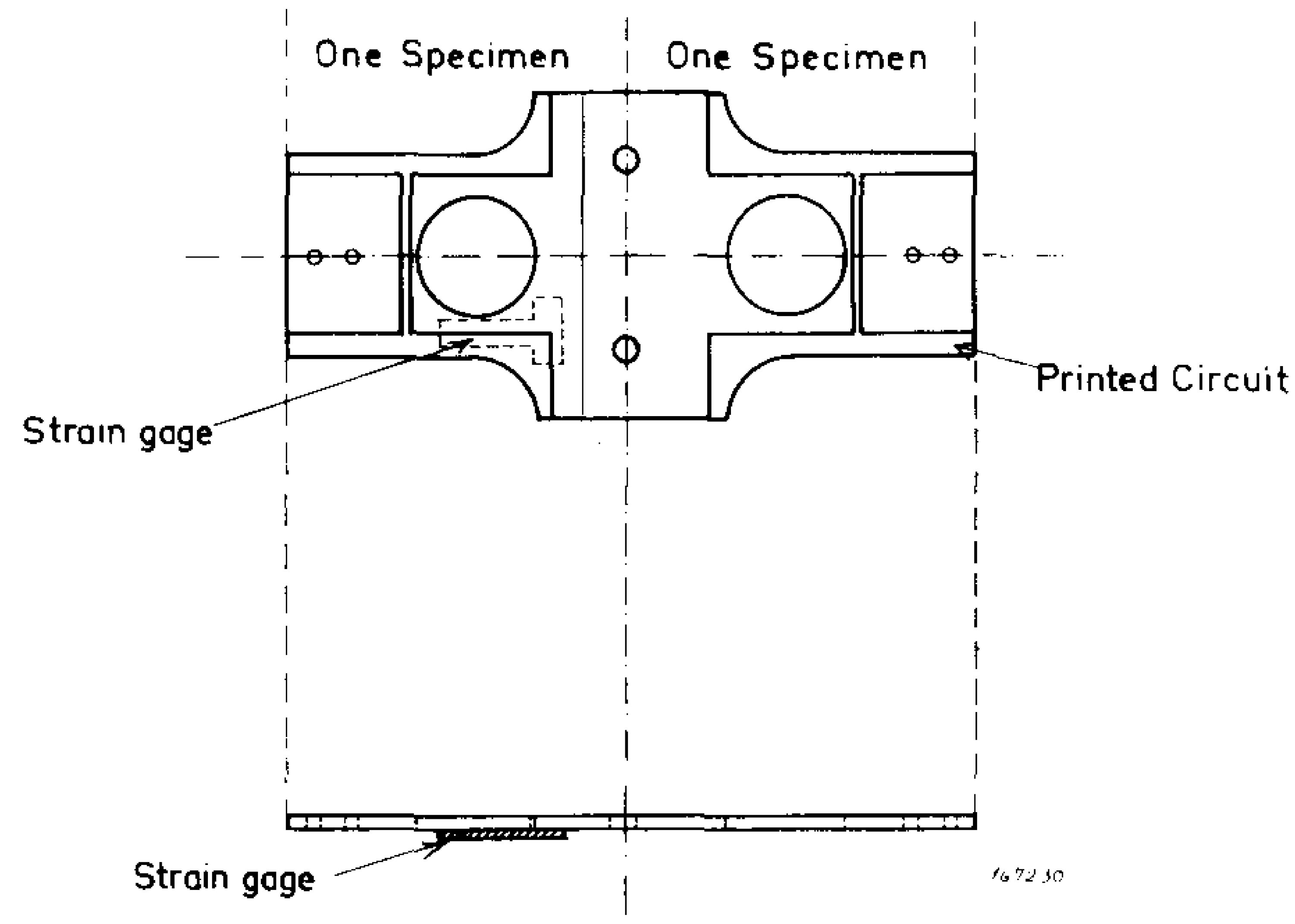

Fig. 13. Sketch of the printed circuit board indicating the position of the strain gage.

so similar that a number of specimens could be tested simultaneously in a test jig, setting the test level from strain measurements on one of the specimens only.*)
Fig. 14 shows a photograph of the specimen arrangements. The boards were fixed to the test jig at its middle whereby each board constituted two specimens as shown. Three boards, i.e. six specimens were tested simultaneously, Fig. 15. Failure in the specimen was detected by the simple fact that the failure of the specimen coincided with breaking of the printed circuit. Thus detection could be carried out by inserting the print in an electrical circuit.

The Experimental Test Arrangement
The experimental test set-up is shown in Fig. 16 and can be split into four separate sections, with regard to the functions they carry out. These functions are the inducement of vibrations in the specimens, the measurement of the induced strain and magnitude of the acceleration level at the vibration table, and the detection of failure in the specimen.

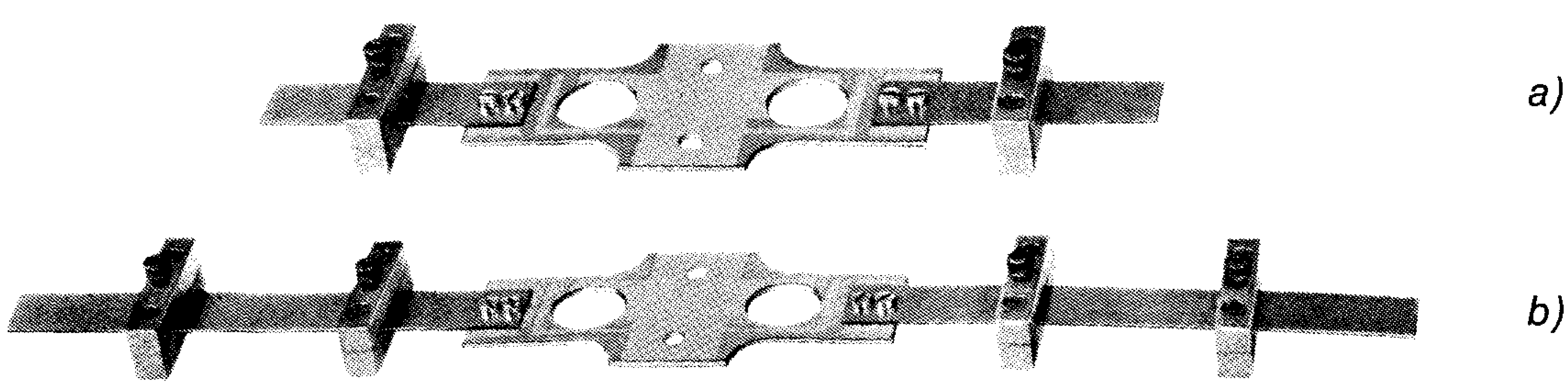

Fig. 14. Photograph of the actual test specimens.
a) The single degree-of-freedom specimen arrangement.
b) The two degrees-of-freedom specimen arrangement.

*) This was later confirmed by strain measurements on all specimens in one group, see Appendix C.

1. Inducement of Vibration:
The vibrations were induced in the specimens by means of an electrodynamic vibrator fed by two Sine-Random Generators Type 1042 with an intermediary stage of a potentiometer and a power amplifier, Fig. 16. The potentiometer was inserted into the circuit to facilitate the adjustment of the final test level.

2. Strain Measurement:
The strain in the specimen was measured by means of a strain gage which was glued to the specimen (see Fig. 13). The gage was inserted into a Wheat-

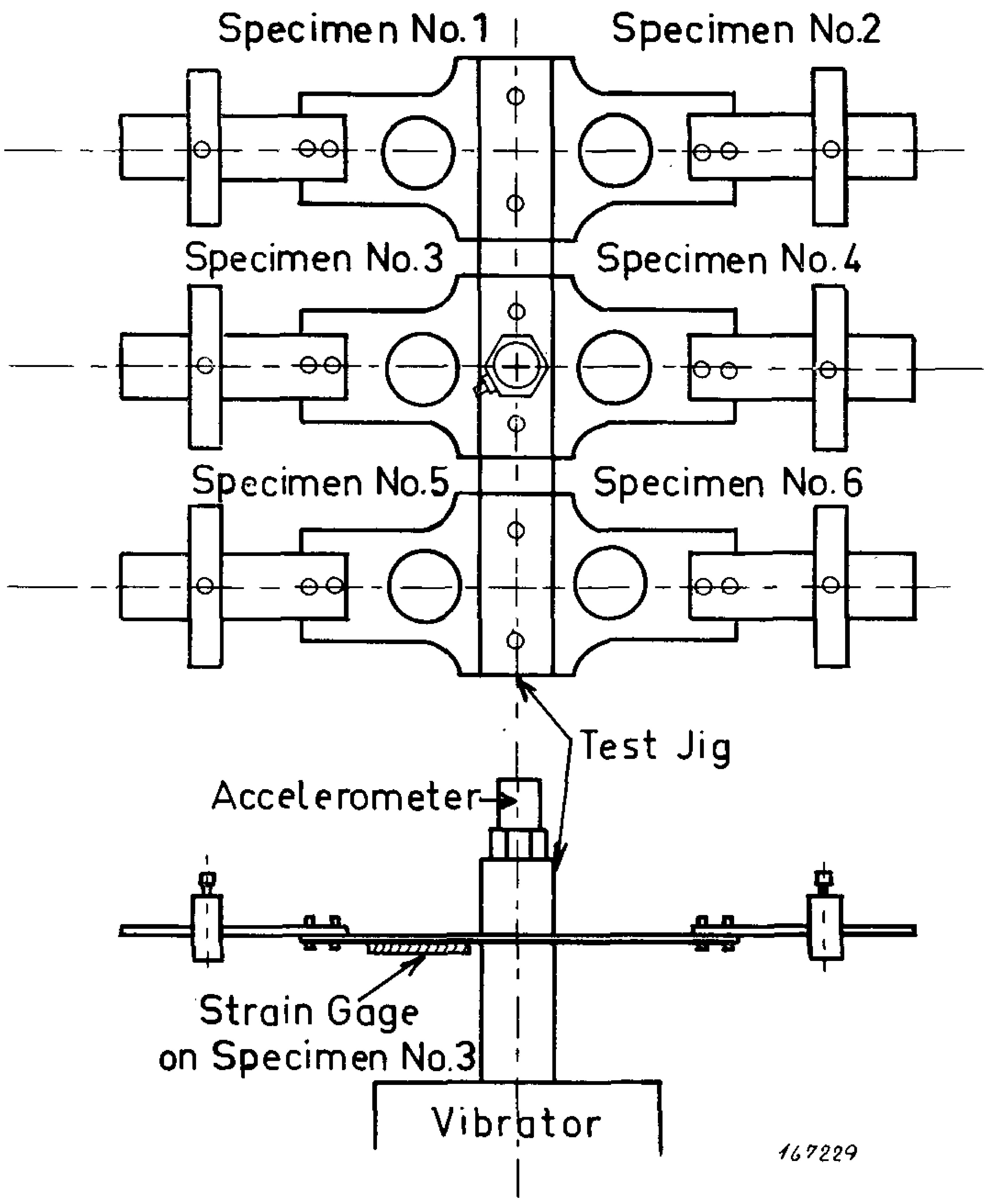

Fig. 15. Sketch of the test jig with one "group" of specimens mounted.

stone bridge arrangement from which the signal passed through a low pass filter and an Audio Frequency Spectrometer Type 2112. It was then measured on a Random Noise Voltmeter Type 2417 and recorded on a Level Recorder Type 2305, Fig. 16.
A constant RMS strain level was maintained throughout the series of tests by adjusting the test level to a certain meter deflection on the Random Noise Voltmeter. A secondary measure of the test level was obtained by means of the Level Recorder which allowed a written record to be produced for comparison purposes.

One possible snag in the system is the performance of the strain gage. This was taken care of in two ways. The first was that the adhesion of the strain gage was carried out with strict adherence to the instructions given by the manufacturer. The second was a static strain gage test. This involved observing the strain, produced by small weights hung on the specimen, measured by the strain gage, and read from a Strain Gage Apparatus Type 1516. The test was carried out for three separate weights and a record kept of these strains which enabled corrections to be made for differences in the strain

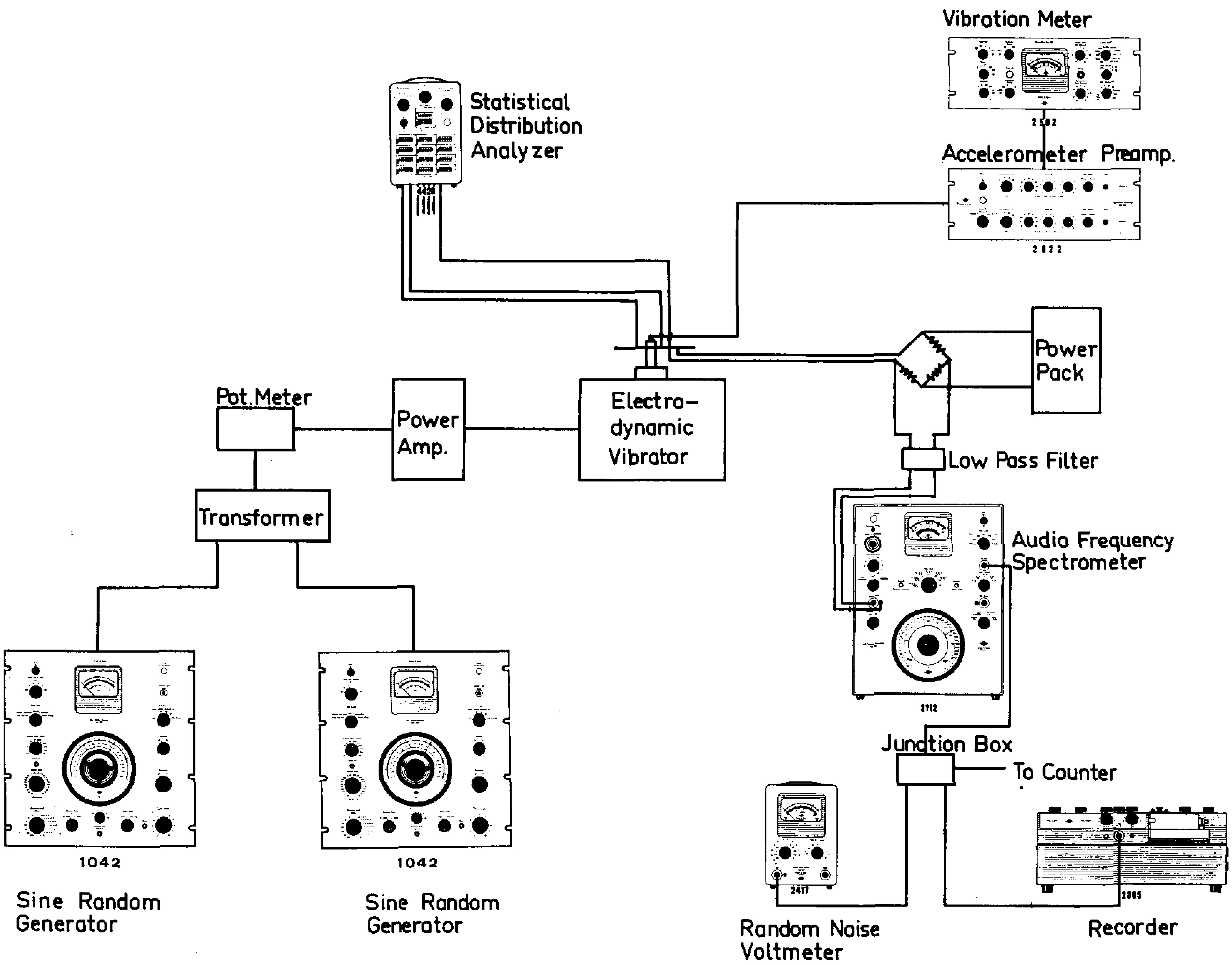

Fig. 16. Block diagram of the experimental test set-up.

gage signal used to set the test level. Another aspect of this test was that it predicted whether or not a gage would "slip" under test conditions (i.e. within the time required for the setting of the test conditions).

3. Acceleration Measurements:

The strain gages provided an excellent method for the initial setting of test level but unfortunately their own fatigue life was far shorter than those of the specimens. This necessitated the use of an accelerometer on the vibration table, as a means by which any "drift" in the apparatus could be detected and corrected. The accelerometer was placed above the centre specimen and

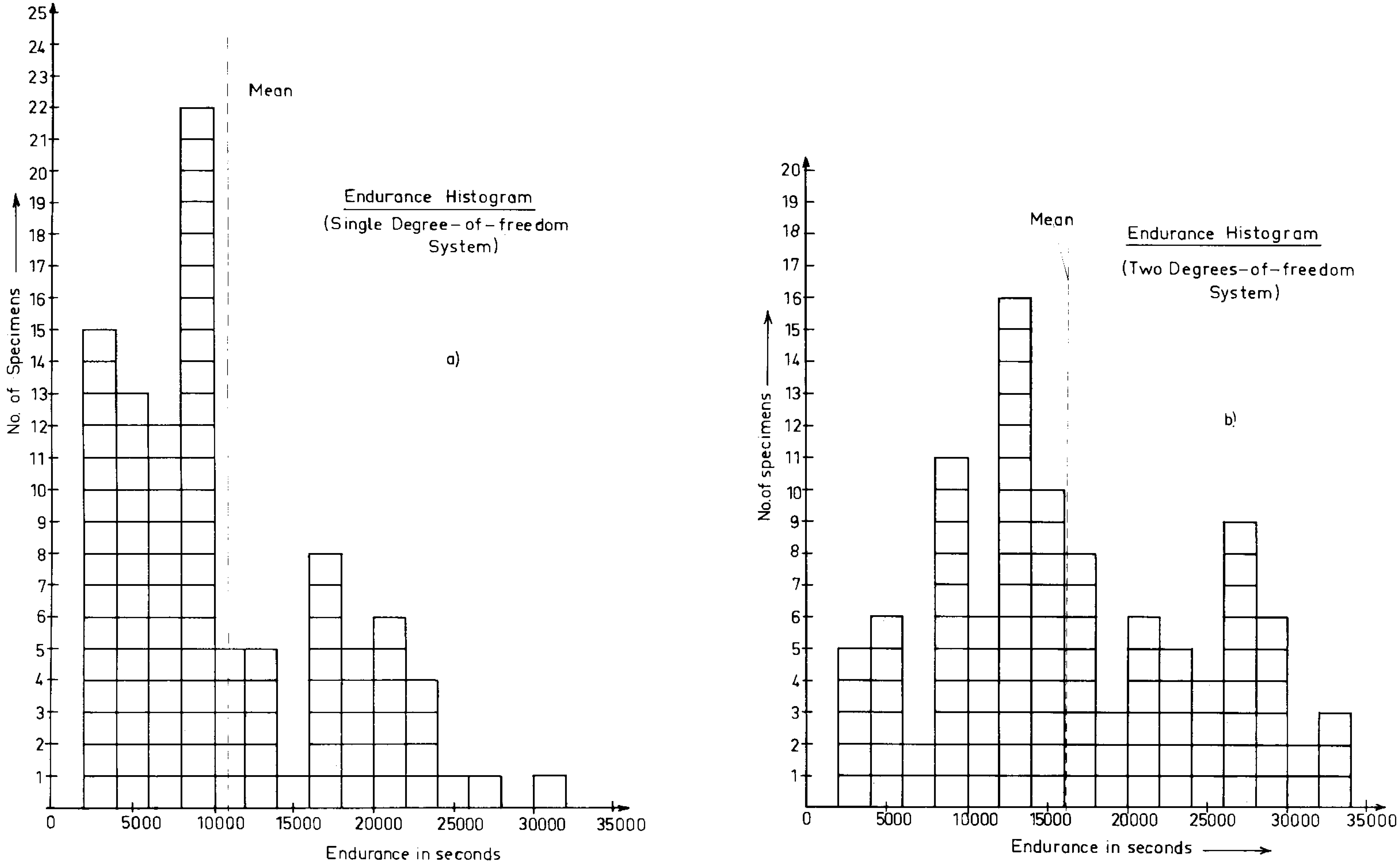

Fig. 17. Fatigue endurance histograms.
a) The single degree-of-freedom test.
b) The two degrees-of-freedom test.

Single degree-of-freedom test			
Rank	Sec's	Rank	Sec's
1	2095	51	8615
2	2095	52	8616
3	2204	53	8665
4	2239	54	8689
5	2411	55	8695
6	2414	56	9016
7	2811	57	9053
8	2820	58	9394
9	2886	59	9397
10	2996	60	9533
11	3046	61	9558
12	3086	62	9688
13	3124	63	9880
14	3501	64	10430
15	3734	65	10490
16	4078	66	10723
17	4130	67	10829
18	4136	68	11206
19	4177	69	12529
20	4276	70	12550
21	4421	71	12806
22	4426	72	13014
23	4717	73	13277
24	4956	74	15915
25	5223	75	16140
26	5459	76	16232
27	5742	77	16418
28	5807	78	16638
29	6058	79	17062
30	6143	80	17787
31	6194	81	17843
32	6194	82	17928
33	6202	83	18093
34	6640	84	18292
35	6657	85	19106
36	6661	86	19133
37	7566	87	19200
38	7614	88	20462
39	7815	89	20796
40	7984	90	20925
41	8016	91	21010
42	8133	92	21333
43	8190	93	21937
44	8225	94	22000
45	8226	95	22220
46	8355	96	22381
47	8357	97	23680
48	4387	98	24281
49	8493	99	27868
50	8616	100	30162

Two degrees-of-freedom test			
Rank	Sec's	Rank	Sec's
1	2965	51	14993
2	3075	52	15303
3	3125	53	15449
4	3421	54	15545
5	3720	55	15582
6	4169	56	15916
7	4321	57	16092
8	4353	58	16125
9	5641	59	16638
10	5727	60	17008
11	5756	61	17287
12	6316	62	17506
13	6389	63	17674
14	8014	64	17810
15	8050	65	18206
16	8120	66	18229
17	8145	67	19728
18	8200	68	20045
19	8231	69	20170
20	8265	70	20675
21	8906	71	21457
22	9202	72	21879
23	9718	73	21883
24	9976	74	22034
25	10362	75	22329
26	10390	76	22694
27	11353	77	23629
28	11442	78	23663
29	11516	79	25070
30	11772	80	25167
31	12316	81	26022
32	12339	82	26055
33	12357	83	26309
34	12475	84	26425
35	12570	85	26865
36	12669	86	26987
37	13115	87	27620
38	13160	88	27857
39	13250	89	27895
40	13251	90	28000
41	13330	91	28086
42	13497	92	28991
43	13707	93	29159
44	13795	94	29245
45	13823	95	29775
46	13981	96	31003
47	14014	97	31311
48	14261	98	32277
49	14483	99	32541
50	14719	100	32891

Fig. 18. Table of the ranked endurance data.

the signal was fed through an Accelerometer Preamplifier Type 2622 to a Vibration Meter Type 2502.

4. Detection of Failure:
Failure detection was established by inserting a Statistical Distribution Analyzer Type 4420 into an electrical circuit including the print on the specimen board. The Distribution Analyzer was switched to operate as a 6-channel time measuring device with a one second time resolution. When the test level was set the counter was started and when failure occurred the printed circuit would break and the counter would stop automatically. Trouble was not experienced with any "remaking" of contact by the printed circuit after failure because the weights used on the end of the specimens kept the circuit open.

Evaluation of the Test Results
Two hundred specimens were tested, one hundred in the form of single degree-of-freedom systems and one hundred in the form of two degrees-of-freedom systems. Histograms of the test results are shown in Fig. 17 while the table Fig. 18 shows the ranked endurance data. To allow trends in the results to show up as early as possible, and to outrule systematic errors in the test set-up, a number of tests were first run on the two degrees-of-freedom system, then on the single degree-of-freedom system, then on the two degrees-of-freedom system again and so forth. This method of testing also allowed a very useful graph to be produced during the test which clearly indicated the trends, see Fig. 19. Here the statistical mean value of the endurance is calculated and plotted as a function of the number of specimens actually

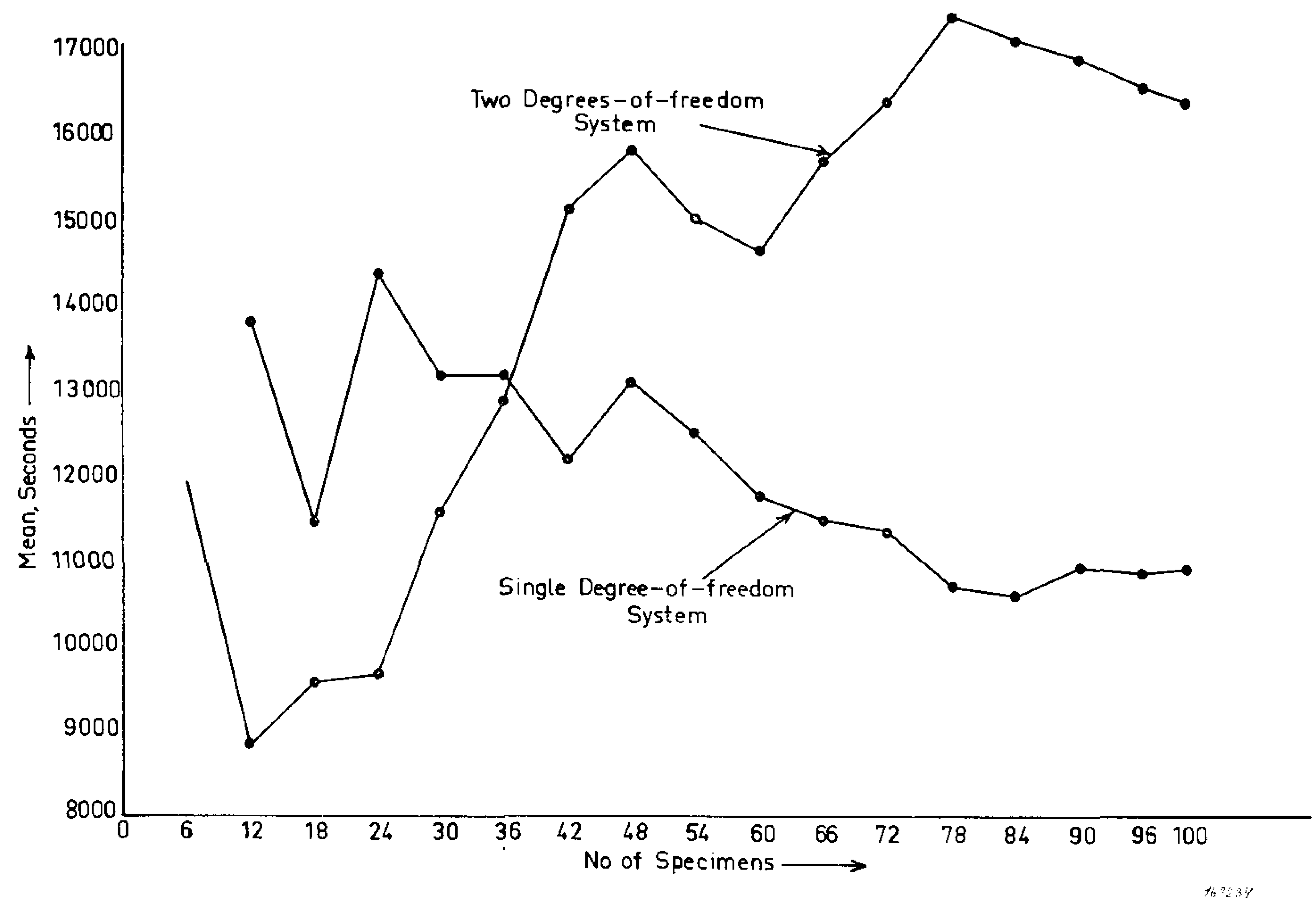

Fig. 19. Mean values of the endurances plotted versus the number of specimens tested.

tested, i.e. after each test run a "correction" could be applied to the previously calculated mean value. The graph shows the erratic variation of the sample mean with only small samples then goes on to the final clarification of the two tests in the manner of a greater uniformity of the sample means with increasing sample size. This plot also shows the reason for the sample size used in the experiment. At the larger sizes the means show a marked tendency for random variations about some central means which should in theory degenerate into straight lines as the sample size approaches infinity. The values of the means at this point would then be the true population means. This plot also clearly demonstrates the difference between the two sample means.

To further ensure statistical significance of the results various techniques might be used. However, because the sample sizes in this case are rather large (100 specimens) the simple "variation of the mean" test is applicable. This test is based on the fact that the mean of any sample of a population is only an estimate of the mean of the true population, and, as can be shown mathematically*) *the standard deviation of the mean is:*

$$\sigma_m = \frac{\sigma_s}{\sqrt{N}}$$

where σ_m = standard deviation of the mean
σ_s = standard deviation of the sample
N = number of items in the sample

The actual values of the means and standard deviations for the two tests concerned are tabulated below.

	Mean	σ_s	σ_m
Single degree-of-freedom test	10902 seconds	7206 seconds	721 seconds
Two degrees-of-freedom test	16330 seconds	8336 seconds	834 seconds

As the difference between the two mean values is *larger than six standard deviations of the mean* it must be concluded that the difference in endurance between the two tests is statistically *highly significant.*

To physically explain the difference in endurance it is necessary to consider for a moment the waveforms of the stress signals in terms of frequency spectra and peak distributions. The frequency spectra for the two stress functions were shown in Fig. 12 and the normalized peak distribution functions are plotted in Fig. 20. The latter can either be calculated from the spectra

*) See for instance P. G. Hoel: "Introduction to Mathematical Statistics", Third Edition, p. 143.

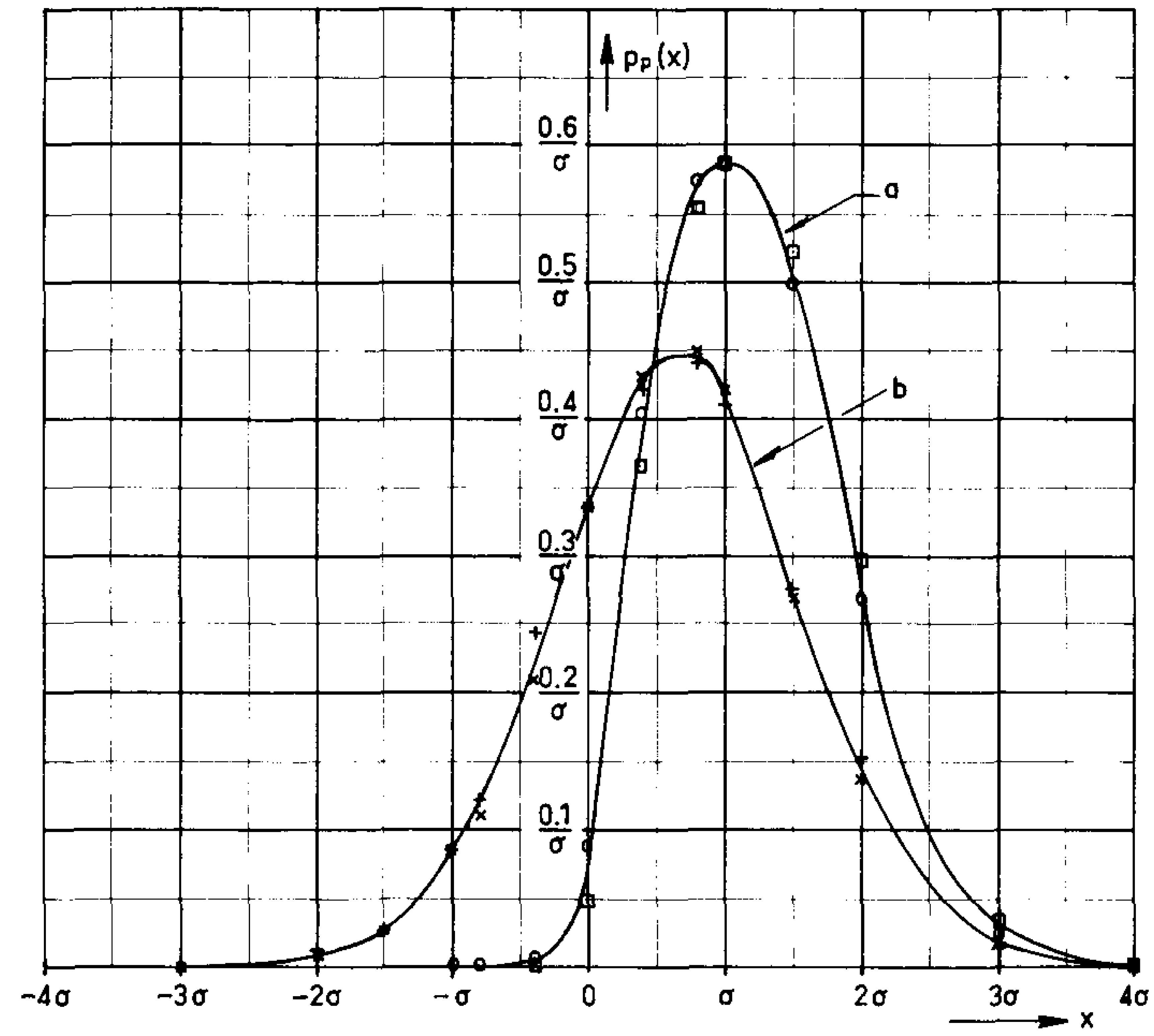

Fig. 20. Normalized peak probability density curves of the measured strain signals.
a) Curve obtained from measurements on the single degree-of-freedom system ($\alpha \approx 1$).
b) Curve obtained from measurements on the two degrees-of-freedom system ($\alpha \approx 0.275$).

by means of the "box"-theory or measured directly from magnetic tape recordings, see Appendix B.

In the case of the single degree-of-freedom system the frequency spectrum shows only one "peak" indicating that the signal consists basically of a single "wave". The corresponding peak distribution curve also indicates that vibration maxima occur practically only on the "positive" side of the zero signal line (and consequently, vibration minima occur only on the "negative" side of the zero signal line!). From the theory of resonating systems it is then clear that between two successive high level stress maxima relatively large vibration strokes occur (see also Fig. 9a). Such a stroke will cause a once started fatigue crack to open and produce a considerable stress concentration at the crack tip, which again may cause the crack to grow.

In the case of the two degree-of-freedom system, on the other hand, the frequency spectrum shows two distinct "peaks", indicating that the signal contains basically two superimposed "waves". From the corresponding peak distribution curve it is seen that here some vibration maxima occur also on the "negative" side of the zero signal line. This again means that some vibration *minima* occur on the "positive" side of the zero signal line. Consequently no *large* vibration strokes *need* to occur between two successive high level stress maxima. That this actually is the case is confirmed by looking at Fig. 9b). The *change* in stress at the fatigue crack tip may therefore be considerably less in this case than in the single degree-of-freedom case even

though the stress level at which the two successive maxima occurs might be the same in both cases. Or said in other words: Even though the *number* of high level stress maxima is the same in the single degree-of-freedom and in the two degrees-of-freedom cases (see Appendix C) the changes in stress at the fatigue crack tip "per maximum" may be widely different.
The ideas outlined here, may at least to a certain extent, explain the difference in fatigue life experienced between the single degree-of-freedom and the two degrees-of-freedom tests described above.
Before finishing the discussion of the test results the possible effects of the difference in static loading between the single degree-of-freedom and the two degress-of-freedom test systems mentioned on p. 13 should be touched upon. Because this difference was very small (10 % of the RMS-value of the dynamic load) it is not deemed to upset the results to any extent. If, on the other hand, it did have any influence at all it has brought the mean values of the two tests closer together, as the two degrees-of-freedom system had the largest static load.

Conclusion

The tests discussed in this paper have been carried out to demonstrate, in a simple way, some effects of randomly superimposed "waves" upon the fatigue life of mechanical constructions. From the results it seems clear that various factors will affect the fatigue life of the construction when this is exposed to complex random loads, even if the loads are Gaussian and the construction behaves linearly. Some of these factors are the RMS-value of the stress, the "average" zero-crossing frequency, the peak distribution factor, α, and, in the case of two degrees-of-freedom systems, also the frequency ratio between the two resonances. When the construction becomes more complicated (multimodal) further factors become involved. On the other hand, it might when practical experiments have been made, turn out that a number of these factors could be neglected. Further work along the lines outlined in this paper is necessary, however, before firm conclusions in this respect can be drawn.

Acknowledgement

The author would like to express his thanks to Mr. J. G. Kershaw for his valuable assistance and interest in carrying out the practical testing.

Appendix A

Estimation of Zero-Crossing Frequency by Means of the "Box"-theory

As mentioned in the text, and further detailed by the author in the B & K Technical Review No. 3-1963, the so-called "box"-theory can, under certain circumstances, be used to estimate normalized peak probability density curves from a knowledge of the frequency spectrum of Gaussian random signals. Similarly, the "box"-theory may also be used to estimate the average zero-crossing frequency of the signal.

Starting with Rice's exact expression for the expected number of zeros per second and using his terminology one can write:

$$2\ f_o = \frac{1}{\pi}\left[-\frac{\Psi_o^{11}}{\Psi_o}\right]^{1/2} = 2\left[\frac{\int_0^\infty f^2\ w(f)df}{\int_0^\infty w(f)df}\right]^{1/2}$$

where f_o is the average zero-crossing frequency and $w(f)$ is the power spectral density of the signal.

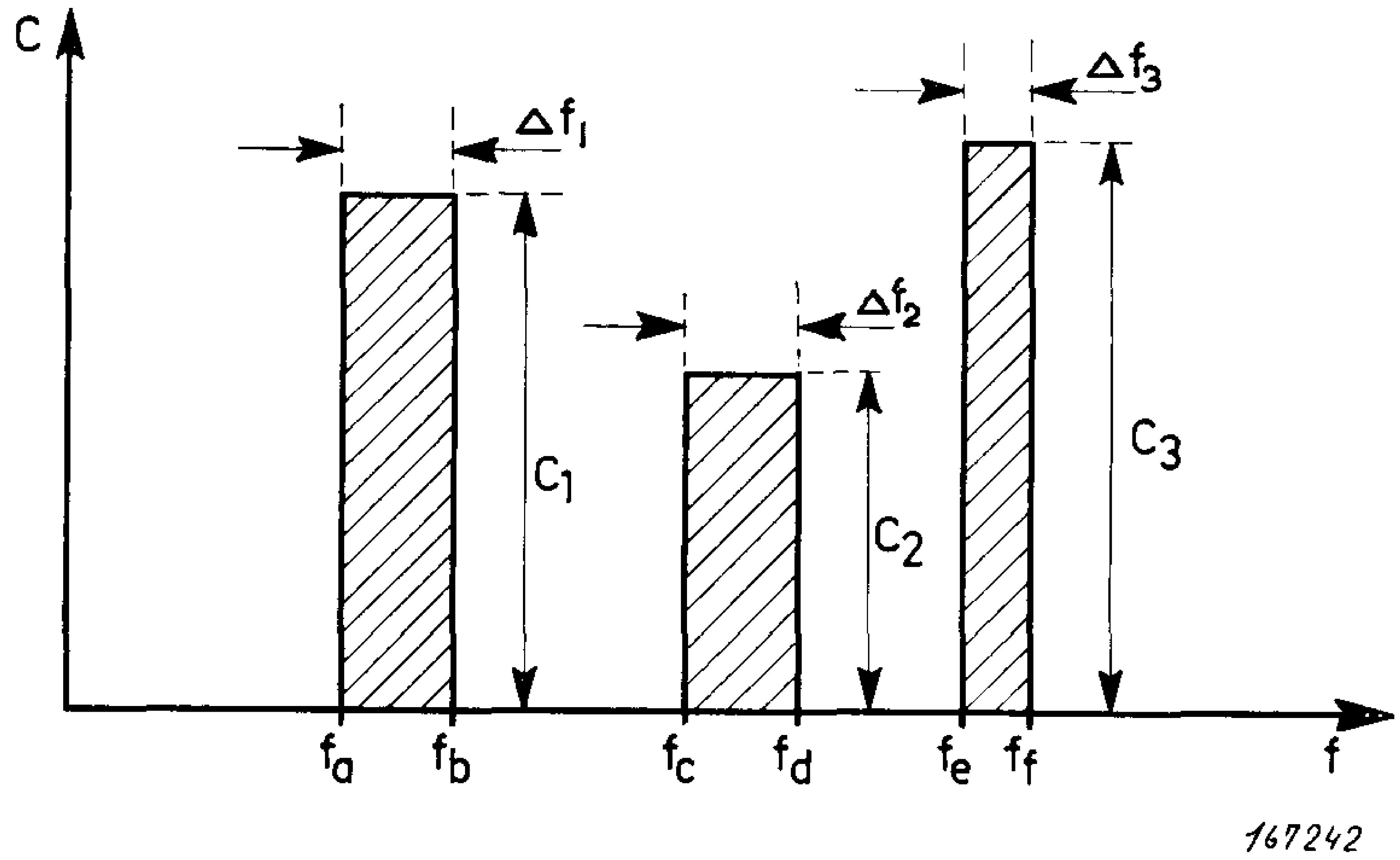

Fig. A.1.

To derive a general "box"-approximation formula for f_o in the case of multi degrees-of-freedom systems consider Fig. A.1. The expressions for Ψ_o and Ψ_o^{11} become:

$$\int_0^\infty w(f)df = \int_{f_a}^{f_c} c_1 df + \int_{f_c}^{f_d} c_2 df + \int_{f_e}^{f_f} c_3 df + \ldots$$

$$= \Delta f_1\ c_1\left(1 + \frac{\Delta f_2\ c_2}{\Delta f_1\ c_1} + \frac{\Delta f_3\ c_3}{\Delta f_1\ c_1} + \ldots\right)$$

$$= \Delta f_1\ c_1\ (1 + \beta_2 + \beta_3 + \beta_4 + \ldots)$$

$$\Psi_o = \Delta f_1\ c_1\ (1 + \sum_2^n \beta_n) = \Delta f_1\ c_1 \sum_1^n \beta_n$$

where the meaning of Δf_1, c_1, Δf_2 etc. can be seen from Fig. A.1 and

$$\beta_n = \frac{\Delta f_n\ c_n}{\Delta f_1\ c_1}$$

Similarly:

$$\Psi_o'' = -4\ \pi^2 \int_0^\infty f^2\ w(f)df = -4\ \pi^2\ (\int_{f_a}^{f_b} f^2 c_1 df + \int_{f_d}^{f_c} f^2 c_2 df + \ldots)$$

$$= -\frac{4\ \pi^2}{3}[c_1\ (f_b^3 - f_a^3) + c_2\ (f_d^3 - f_c^3) + c_3\ (f_f^3 - f_e^3) + \ldots]$$

According to Fig. A.1:

$$f_b = f_a + \Delta f_1 \quad ; \quad f_d = f_c + \Delta f_2 \quad ; \quad \dots$$

Thus:

When $\frac{\Delta f_1}{f_a}$ is very small (lightly damped resonance) then $\left(1 + \frac{\Delta f_1}{f_a}\right)^3$

$$\approx 1 + 3 \frac{\Delta f_1}{f_a}$$

whereby

$$f_b^3 - f_a^3 \approx 3 f_a^2 \, \Delta f_1 \quad ; \quad f_d^3 - f_c^3 \approx 3 f_c^2 \, \Delta f_2 \quad ; \quad \dots$$

Also, in this case no great error is introduced by setting $f_a = f_1$, $f_c = f_2$, $f_e = f_3$, etc. where $f_1, f_2, f_3 \dots$ are the center frequencies of the different resonances. Using these approximations the expression for Ψ^{11} becomes:

$$\Psi_o^{11} = -4\pi^2 \, \Delta f_1 \, c_1 \, f_1^2 \left(1 + \sum_2^n \left(\frac{f_n}{f_1}\right)^2 \beta_n\right)$$

$$= -4\pi^2 \, \Delta f_1 \, c_1 \, f_1^2 \sum_1^n \left(\frac{f_n}{f_1}\right)^2 \beta_n$$

By inserting Ψ_o and Ψ_o^{11} into Rice's formula for f_o one obtains:

$$f_o = \frac{1}{2\pi} \sqrt{-\frac{\Psi_o^{11}}{\Psi_o}} = f_1 \sqrt{\frac{\sum_1^n \left(\frac{f_n}{f_1}\right)^2 \beta_n}{\sum_1^n \beta_n}}$$

Applied to the two degrees-of-freedom system this gives:

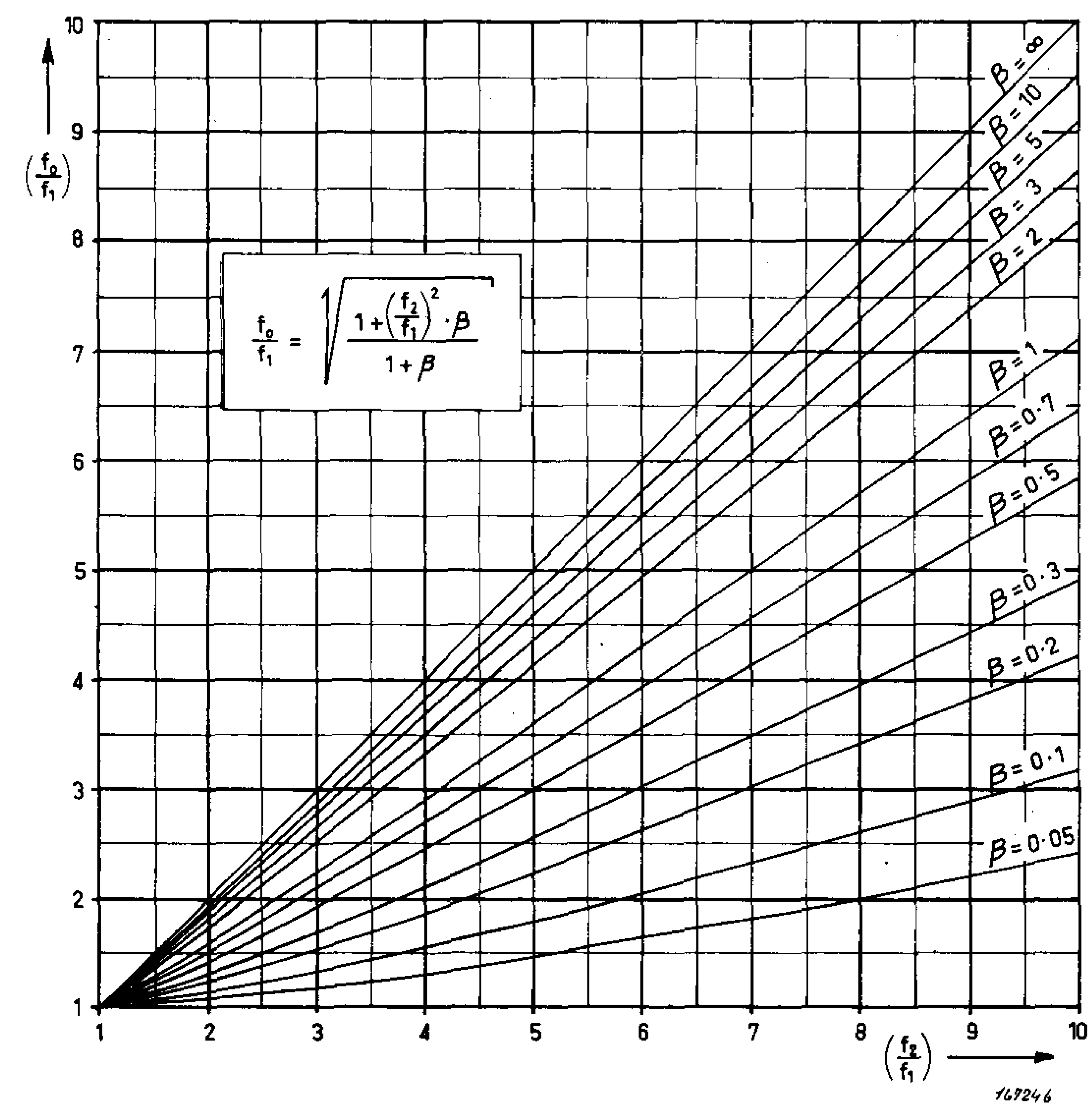

Fig. A.2.

$$f_o = f_1 \sqrt{\frac{1 + \left(\frac{f_2}{f_1}\right)^2 \beta}{1 + \beta}}$$

In Fig. A.2 the ratio $\frac{f_o}{f_1}$ is plotted against $\frac{f_2}{f_1}$ with β as parameter.

Appendix B

Determination and Measurement of Probability Density Data

In the case of the single degree-of-freedom system the normalized peak probability density curve should theoretically follow, very closely, the so-called Rayleigh probability density function. That this actually is the case can be seen from Fig. 20 of the text.

To determine the peak probability density curve for the two degrees-of-freedom system, two methods can be used. Either the α-value for the distribution can be determined from the frequency spectrum, Fig. 12b), and the corresponding normalized probability density function plotted, or the curve can be measured directly from magnetic tape recordings of the strain. Both methods are demonstrated in the following.

An estimate of the α-value from the frequency spectrum can be made by means of the "box"-theory as follows:

The frequency ratio between the two resonances is approximately (see Fig. 12b):

$$\frac{f_2}{f_1} \approx 6 = 2.6 \text{ octaves}$$

As the frequency analysis data were obtained by means of a constant percentage bandwidth analyzer a "correction" of $2.6 \times -3\text{ dB} = -7.8$ dB must be applied to the data.

The level difference between the two resonance peaks, as read from the spectrum, is approximately -5.5 dB. Together with the above mentioned "correction" this gives $-(7.8 + 5.5) = -13.3$ dB.

Because the Q-values of the two resonances are of the same order of magnitude, and because the frequency analysis was performed as constant percentage bandwidth analysis, no correction need be considered for the bandwidth ratio, which is then found to:

$$\frac{\Delta f_2}{\Delta f_1} = \frac{170}{26} = 6.55$$

The total energy ratio (β) is thus:

$$\beta = \frac{6.55}{21.4} = 0.306$$

as -13.3 dB corresponds to a ratio of $\frac{1}{21.4}$

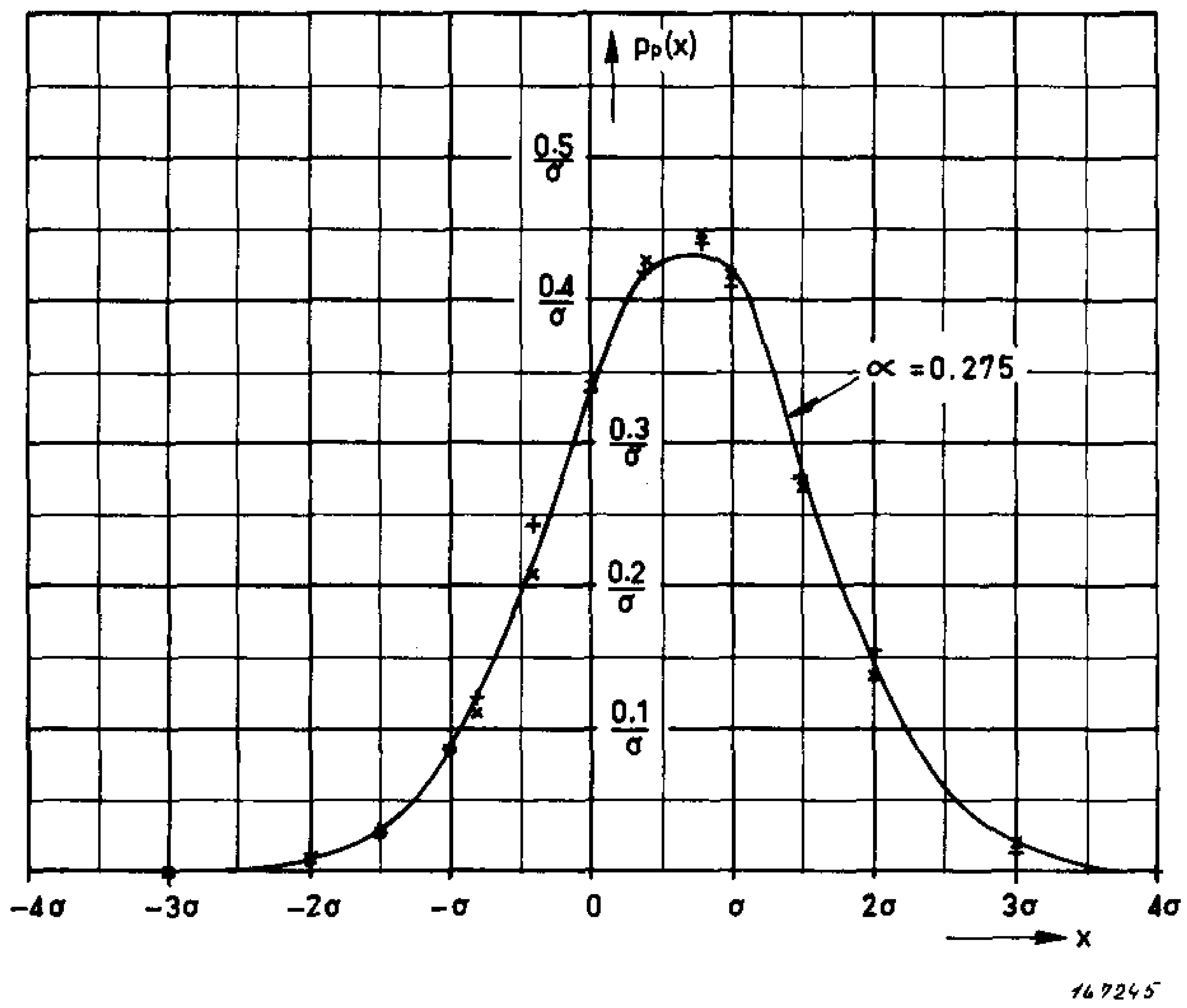

Fig. B.1.

It is now an easy matter to find α from the formula (see also p. 8):

$$\alpha = \frac{\left[1 + \left(\frac{f_2}{f_1}\right)^2 \beta\right]^2}{\left[1 + \beta\right]\left[1 + \left(\frac{f_2}{f_1}\right)^4 \beta\right]} = \frac{(1 + 36 \times 0.3)^2}{1.3\ (1 + 36 \times 36 \times 0.3)} \quad \text{ɔ}: \alpha = \mathbf{0.275}$$

The normalized peak probability density curve for $\alpha = 0.275$ is plotted in Fig. B.1 and compared to measured (and normalized) data.
Probability density measurements on tape recorded data of the strain signal were made by means of a sligtly modified Probability Density Analyzer Model 161, see Fig. B.2. The "window"-width of the Analyzer was adjusted to 0.15 σ and the hysteresis in the "window" flip-flops were given the same value to avoid extraneous, very low level noise disturbance. An original sample duration of 400 seconds was used, which by a forty-to-one tape speed transformation was reduced to 10 seconds.

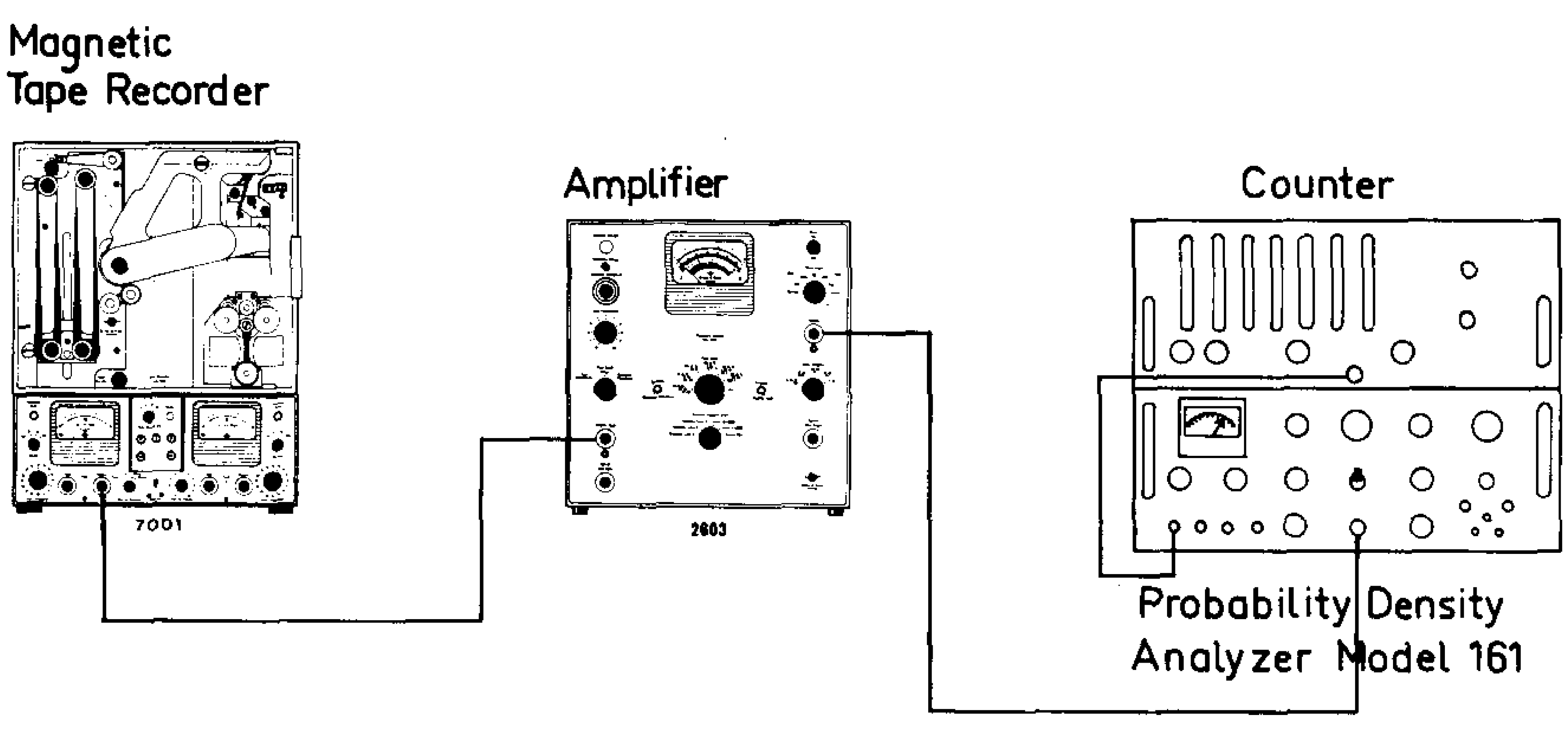

Fig. B.2.

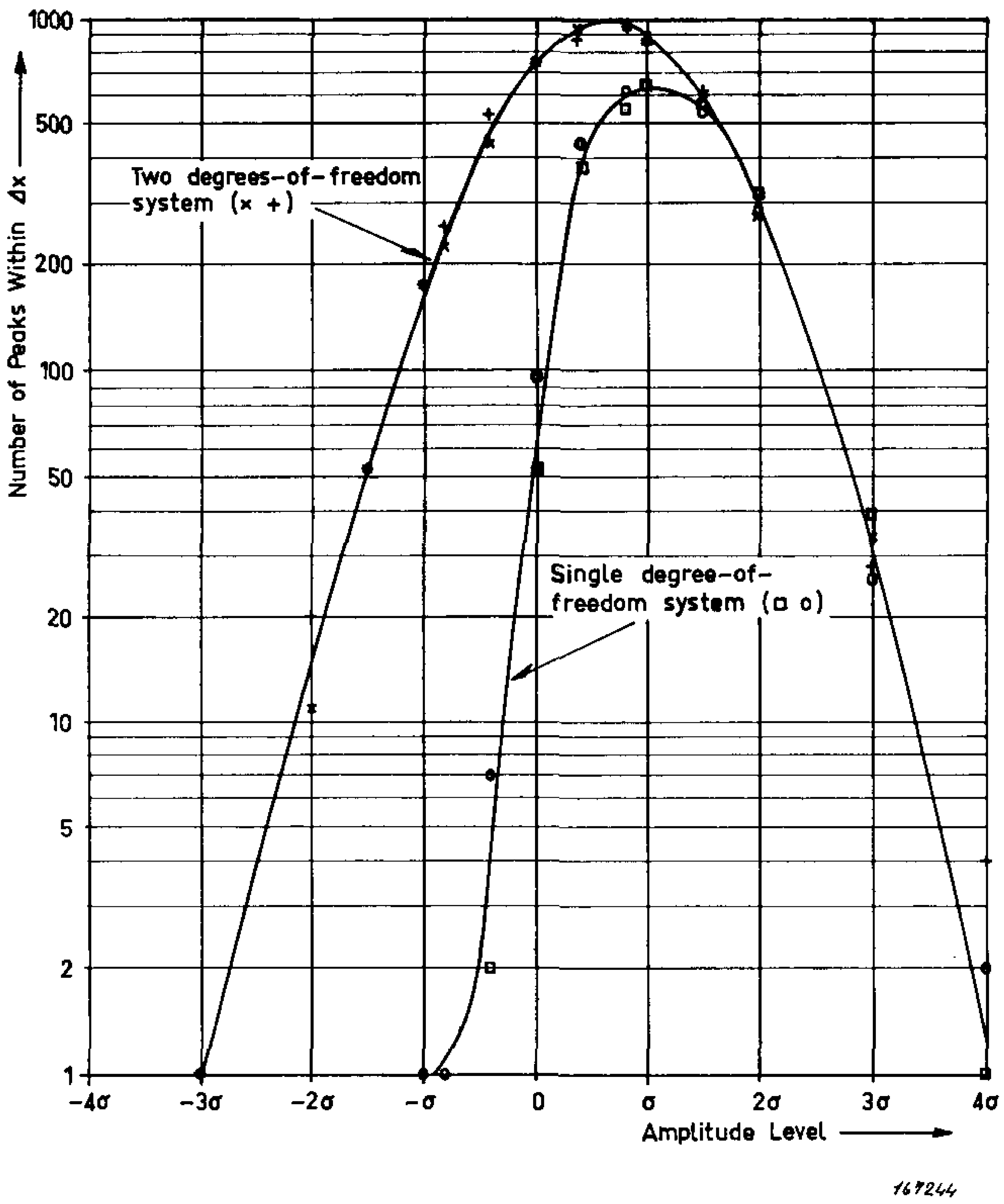

Fig. B.3.

The actually measured number of strain maxima are plotted in Fig. B.3 to a logarithmic scale, both for the two degrees-of-freedom and for the single degree-of-freedom test. Due to the limited duration of the samples it should be noted, however, that the statistical accuracy of the data is also limited. Data from two samples of each test are tabulated below.

Also the first order probability density curve was measured in both cases. The results of the measurements are shown in Fig. B.4 and compared with the normal Gaussian curve.

		4 σ	3 σ	2 σ	1.5 σ	σ	0.8 σ	0.4 σ	0	-0.4 σ	-0.8 σ	- σ	-1.5 σ	-2 σ	-3 σ
Single degree-of-freedom test	Sample 1	2	25	288	537	638	618	435	96	7	1	1	–	–	–
	Sample 2	1	38	320	563	635	546	378	52	2	–	–	–	–	–
Two-degrees-of-freedom test	Sample 1	0	33	277	569	888	956	921	720	445	228	176	52	11	1
	Sample 2	4	27	305	604	870	941	896	717	516	255	180	53	20	1

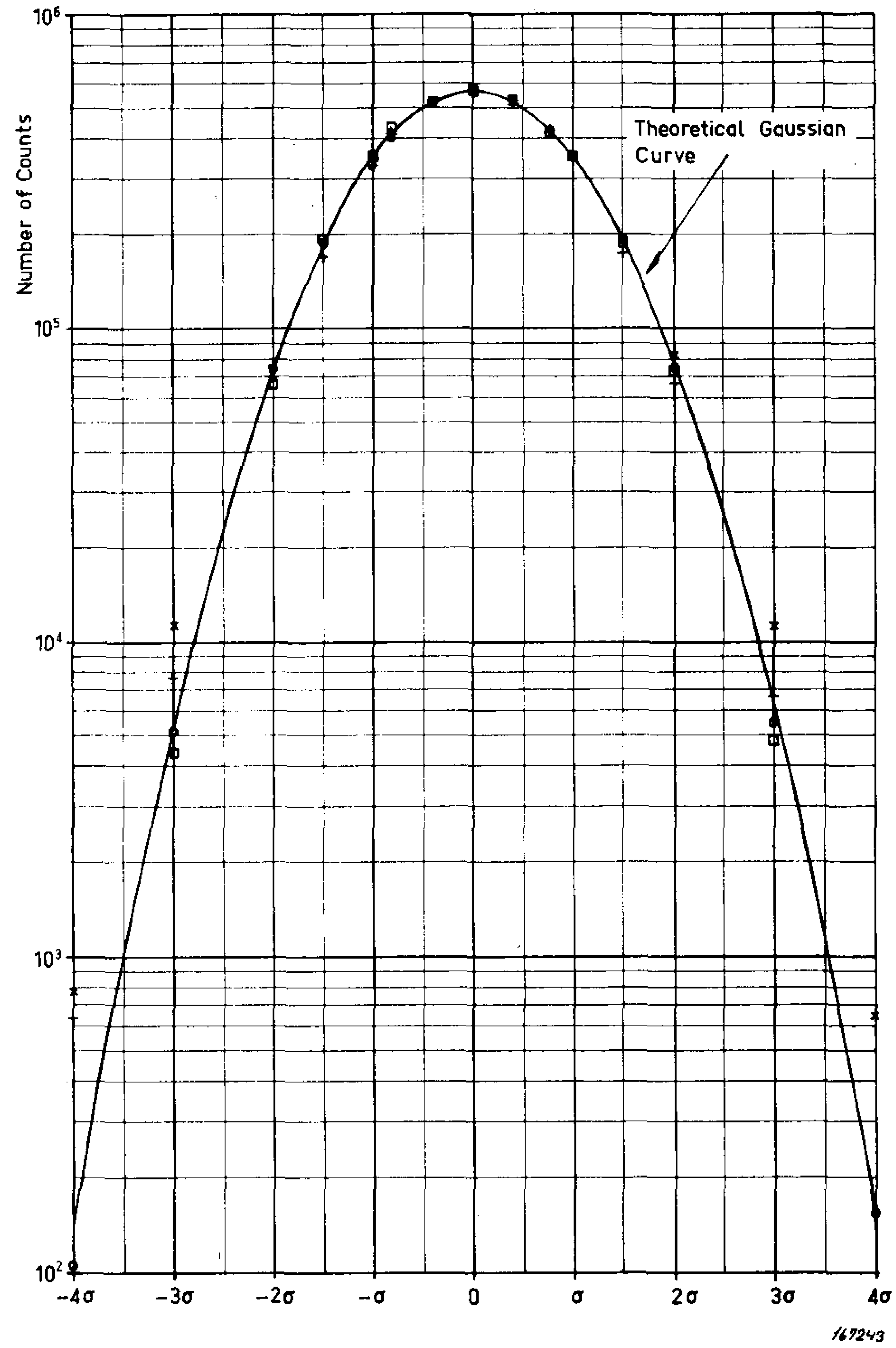

Fig. B.4.

Appendix C

Variation in Strain Between Specimens

It was stated in the text that the tests were carried out in groups of six specimens with a strain gage on the centre specimen to set the level. This poses the question of whether the strain in the centre specimen is representative of the strain felt by the other specimens in the group. To clarify this the following experiments were carried out. Strain gages were attached to all six specimens in a group of specimens which were chosen at random from the supply. The static strain gage test (see main text) was then carried out for all six strain gages and the results noted. The specimens were then mounted on the vibration table in the manner used for normal testing and the strain gages wired to a multi switch and connected to the strain measuring equipment of the test set up. A low level random vibration signal was fed into the electrodynamic vibrator.

The signals from the various strain gages were then observed successively on the Level Recorder. The use of a Level Recorder allowed for an easy method of comparison. When the signals from the strain gages had been measured

and recorded the level was increased to the test level and a normal test carried out.
As results of the above described experiment the following was noted:

1) The variation in the response of the strain gages from the static strain test was less than 10 %.
2) The variation in dynamic strain between the specimens when tested on the vibrator was of the order of 1 dB.
3) The variation in average zero crossing frequency between the specimens was less than 2 Hz.
4) The spread in fatigue life was "normal", see table below.

Specimen No.	1	2	3	4	5	6
Fatigue Endurance (Seconds)	9820	5742	18292	19106	8387	4717

From these results it can be concluded that although there may be small variations in the strain from specimen to specimen, the variations observed above are not significant and can be explained from the difference in response of the various strain gages.
The spread in fatigue life also showed that the specimens were not a singular group with an exceptionally uniform character but were a true representation of the specimens used.

References:

BROCH, J. T.: Effects of Spectrum Non-linearities upon the Peak Distribution af Random Signals. Brüel & Kjær Techn. Rev. No. 3-1963.

HAAGENSEN, P. J.: Statistical Aspects of Coexisting Fatigue Failure Mechanisms in OFHC Copper. UTIAS*) Technical Note No. 112, June 1967.

HOEL, P. G.: Introduction to Mathematical Statistics. Third Edition. John Wiley & Sons, Inc. New York – London 1964.

MUGGERIDGE, D. B.: An Attempt to Correlate Bimodal Fatigue Endurance Distributions in OFHC Copper with Wood's H, F and S Ranges. UTIAS*) Technical Note No. 111, June 1967.

RICE, S. O.: Mathematical Analysis of Random Noise. Bell System Techn. Journal 23 (1944) and 24 (1945). Also contained in N. Wax: "Selected Papers on Noise and Stochastic Processes". Dover Publications Inc. New York 1954.

*) University of Toronto Institute of Aerospace Studies.

WEIBULL, W.: A Statistical Representation of Fatigue Failures in Solids. Kungl. Tekniska Högskolans Handlingar No. 27, Stockholm 1949.

WEIBULL, W.: Fatigue Testing and Analysis of Results. AGARD-Publication by Pergamon Press. Oxford – London. New York – Paris, 1961.

WILLIAMS, T. R. G. and MITCHELL, P. G.: Significance of the Discontinuity in S/N Fatigue Curves. University of Southampton ISAV Memorandum No. 118, January 1965.

SWANSON, S. R.: An Investigation of the Fatigue of Aluminium Alloy due to Random Loading. UTIAS*) Report No. 84, 1963.

SWANSON, S. R., CICCI, F. and HOPPE, W.: Crack Propagation in Clad 7079-T 6 Aluminium Alloy Sheet Under Constant and Random Amplitude Fatigue Loading. Paper 37, 69th Annual Meeting of the ASTM, June 1966.

SWANSON, S. R.: Random Load Fatigue Testing: A State of the Art Survey. Paper given on the 70 th Annual Meeting of the ASTM, June 1967.

Brüel & Kjær

ADR.: BRÜEL & KJÆR
NÆRUM - DENMARK

TELEPHONE: 800500
BRUKJA, Copenhagen

TELEX 5316

PRINTED IN DENMARK K. LARSEN & SØN - LYNGBY